

Technische Universität München

Klinik und Poliklinik für Vaskuläre und Endovaskuläre Chirurgie
Klinikum rechts der Isar der Technischen Universität München
(Vorstand: Prof. Dr. Hans–Henning Eckstein)

Chitinase-3-like-Protein-1 and its role in vascular smooth muscle cell survival in advanced atherosclerosis

Shen Lao

Vollständiger Abdruck der von der Fakultät für Medizin der Technischen Universität München zur Erlangung des akademischen Grades eines **Doktors Medizin** genehmigten Dissertation

Vorsitzender: Prof. Dr. Ernst Rummeny

Prüfende/-r der Dissertation:

1. Prof. Dr. Lars Maegdefessel
2. **apl.** Prof. Dr. Christian Hengstenberg

Die Dissertation wurde am 22.07.2019 bei der Technischen Universität München

eingereicht und durch die Fakultät für Medizin am 10.03.2020 angenommen

Abstract

Objectives

In the past decade, stroke-related deaths and disability have increased, making stroke the second leading cause of death and the third leading cause of adult disability worldwide. Given the extensive evidence that vascular smooth muscle cells (VSMCs) play a critical role in both, atherosclerotic plaque development and rupture, a deeper understanding of VSMCs function in advanced atherosclerosis will help with achieving the goal of developing novel diagnostic and therapeutic strategies to prevent plaque vulnerability.

Methods

By performing a Human Transcriptome Array of the fibrous cap in ruptured plaques of symptomatic patients (n=20) vs. stable plaques of asymptomatic patients (n=20), chitinase-3-like protein 1 (CHI3L1) was detected as the most significantly upregulated transcript. In an *ex vivo* study, immunohistochemistry was used to compare the distribution of CHI3L1-positive cells, VSMCs and macrophages in ruptured and stable plaques. In an *in vitro* study, live-cell imaging analysis was implemented to further investigate the effects of CHI3L1 on primary patient-derived VSMC cell survival, migration, proliferation, and apoptosis. Following, Taqman gene expression arrays in CHI3L1-modulated VSMC and *in silico* analysis were performed to investigate promising co-regulators and transcription factors of CHI3L1's involvement in progressing atherosclerosis.

Results

Immunohistochemistry of human carotid plaques demonstrated that expression levels of CHI3L1 in VSMC are increased in ruptured lesions in comparison to stable plaques. Apart from VSMCs, some macrophages also appeared to be CHI3L1-positive, in particular in rupture plaques. In addition, CHI3L1/CD68-positive cells in rupture plaques appeared hyperproliferative (Ki-67 positive). A live-cell imaging analysis showed that silencing Chi3l1 tends to reduce VSMC migration and proliferation, while inducing VSMC apoptosis in primary patient-derived cells. Furthermore, siRNA-guided knockdown of Chi3l1 significantly increased CD68 expression and decreased ACTA2 expression in VSMCs respectively. Meanwhile, the transcription factor Krüppel-like factor 4 (KLF4) was detected as significantly down-regulated in CHI3L1 inhibited VSMCs, suggesting a potential role for CHI3L1 in VSMC phenotypic transition towards a more inflamed, macrophage-like phenotype. In addition, Myogenin (Myog) as the only transcript significantly correlated with CHI3L1 overexpression or inhibition, supporting a role in regulating CHI3L1-mediated VSMC cell fate. Through *in silico* analysis, CAMP Response Element-Binding Protein CRE-BP1 and other nine potential transcription factors were reported and deserved further investigation.

Conclusions

In conclusion, our study supports a role for CHI3L1 in VSMC-mediated plaque vulnerability by regulating VSMC proliferation, migration and apoptosis, while preventing VSMC transformation *via* altered expression patterns of macrophage and VSMC markers through the key regulator KLF4 in VSMC-mediated lesion pathogenesis.

Keyword: Chitinase-3-like-Protein-1 (CHI3L1), stroke, atherosclerosis, vascular smooth muscle cells (VSMCs), proliferation, migration, apoptosis

TABLE OF CONTENTS

1. INTRODUCTION.....	8
1.1 Epidemiology.....	8
1.1.1 Cardiovascular diseases (CVD) and Stroke.....	8
1.1.2 Ischemic stroke and carotid stenosis.....	8
1.2 Etiology and pathogenesis.....	11
1.2.1 Atherosclerosis.....	11
1.2.2 Vulnerable plaque and vascular smooth muscle Cell (VSMCs).....	11
1.2.3 Phenotypic switching of VSMCs in atherosclerosis.....	14
1.3 CHI3L1/YKL-40.....	15
1.3.1 CHI3L1 in preliminary differential Transcriptome array analysis.....	15
1.3.2 CHI3L1 in Identification and characterization.....	17
1.3.3 CHI3L1 in Biology and physiology.....	17
1.3.4 CHI3L1 in atherosclerosis.....	18
1.3.5 Main aims of the doctoral thesis.....	19
2. MATERIALS AND METHODS.....	20
2.1 Munich Vascular Biobank and cell culture.....	20
2.1.1 Munich Vascular biobank.....	20
2.1.2 Carotid artery tissue processing.....	21
2.1.3 Isolation of primary patient-derived vascular smooth muscle cells.....	22
2.1.4 Culture of Primary Patient-Derived VSMCs.....	23
2.1.5 CHI3L1 Recombinant plasmid.....	23
2.1.6 CHI3L1 Knockdown.....	25
2.2 RNA isolation and qRT-PCR.....	25
2.3 Immunohistochemistry.....	26
2.4 Live-cell imaging and analysis.....	27
2.4.1 IncuCyte Live-Cell Analysis System and IncuCyte ZOOM software.....	27
2.4.2 IncuCyte Scratch Wound Assay.....	29
2.4.3 IncuCyte Apoptosis assay.....	29
2.4.4 IncuCyte proliferation assay.....	30
2.5 Prediction of potential mediators of CHI3L1 modulation.....	30
2.6 TaqMan gene expression array.....	31
2.7 Transcription factor prediction.....	33
2.8 Statistical analysis.....	34
3. RESULTS.....	34
3.1 Immunohistochemical analysis of CHI3L1.....	34
3.2 Analysis of CHI3L1 modulation at mRNA level in VSMC.....	36
3.2.1 Efficiency of CHI3L1 modulation in VSMCs.....	36
3.2.2 Exploring role of CHI3L1 in VSMC phenotypic switching.....	38
3.3 CHI3L1 knockdown inhibits migration in VSMCs.....	39
3.4 CHI3L1 knockdown induces apoptosis in VSMCs.....	40
3.5 CHI3L1 knockdown reduces proliferation in VSMCs.....	42

3.6 Potential mediators of CHI3L1 modulation.....	45
3.7 Prediction of transcription factors interacting with CHI3L1.....	46
4. DISCUSSION.....	48
5. SUMMARY.....	51
6. REFERENCES.....	52
7. APPENDIX.....	58
7.1 Abbreviations.....	58
7.2 Publications.....	59
7.2.1 Original publications.....	59
7.2.2 Oral & Poster Presentation.....	59
7.3 Acknowledgments.....	60
7.4 Funding.....	61

1. INTRODUCTION

1.1 Epidemiology

1.1.1 Cardiovascular diseases (CVD) and Stroke

As a result of atherosclerosis, Cardiovascular diseases (CVD) are now the leading cause of mortality and morbidity worldwide (Joseph 2017). According to the latest report from the AHA (American Heart Association), CVD causes 17.9 million deaths per year, and the number has increased globally during the past decade by 12.5%. This number is expected to increase to 23.8 million by 2030 (Benjamin 2018), accounting for approximately one-third of all deaths globally (GBD 2015 DALYs and HALE Collaborators 2015). Over 95% of CVD deaths are attributable to six conditions: stroke, ischemic heart disease, hypertensive heart disease, cardiomyopathy, rheumatic heart disease, and atrial fibrillation (Roth 2015). Furthermore, CVD represents a major socio-economic burden on society.

Over the past 2 decades, stroke has been the second leading contributor to CVDs with 15 million patients suffering a new or recurrent stroke every year (Li 2018). There were 5.9 million deaths annually and nearly 650,000 deaths per year in Europe alone (Go 2014). Meanwhile, the number of stroke-related deaths is still rising each year due to global population growth and the aging population (Hankey 2017). There were also an additional 5 million patients left permanently disabled due to a stroke, making it the third leading cause of adult disability worldwide. This global burden can be expressed as years of life lost and years lived with disability, placing a large socioeconomic burden on society. Thus, better diagnosis and treatment of strokes requires a deep understanding of their epidemiology, etiology, pathogenesis, and molecular characteristics.

1.1.2 Ischemic stroke and carotid stenosis

A stroke is the sudden loss of neurological function due to the interruption of blood supply to the brain (Caplan 2009). There are two major classifications of brain damage in stroke patients: ischemic and hemorrhagic stroke, which are caused by an abrupt occlusion of an artery or bleeding into brain when a blood vessel ruptures, respectively. The consequences of a stroke depend on its severity and the area of the brain injured. As different parts of the brain have different functions, strokes can lead to sudden weakness, loss of sensation, or difficulty with speaking or walking.

Accounting for approximately 85% of all strokes (Creager 2004), ischemic strokes are much more common than hemorrhagic strokes. An ischemic stroke is caused by an interruption or blockage in an artery or multiple arteries that transiently or permanently reduces blood flow to the brain. In fact, there are two main mechanisms: embolism and thrombosis. In an embolism, an arterial embolus lodges within the brain from the heart, a carotid artery, or elsewhere within the artery or vein system, blocking blood flow. By comparison, a thrombosis luminal occlusion is caused by a

localized process at the site of an atherosclerotic plaque originating within the artery. Being responsible for 65% of all strokes, thrombosis-plaque-caused arterial obstruction is the major cause of ischemic stroke (Zivin 2012). Figure 1A shows the formation of atherosclerotic plaques, which are deposited within the carotid artery wall in the neck, blocking the free flow of blood. This atherosclerotic process is also called carotid stenosis or carotid artery disease. It is a progressive narrowing of the carotid arteries.

According to a recent clinical trial in the treatment of Acute Ischemic Stroke (AIS) (Li 2016), AIS is more likely to be associated with the rupture of carotid plaque. Around 20% of ischemic strokes appear to originate from carotid plaques. Thus, as being the most common initiator that leads to ischemic stroke (del Zoppo 2006), carotid stenosis is thought to increase the risk of ischemic stroke in a variety of ways. Progressive narrowing of the lumen eventually blocks the artery completely, forming a clot that blocks blood supply to the brain. This clot then ruptures into an embolus and lodges in smaller downstream vessels; blood flow to this part of the brain stops. The most common area of atherosclerotic plaque formation – and consequentially, plaque vulnerability – is the bifurcation, where the common carotid on each side splits into the external and internal carotid arteries, usually at the upper border of the thyroid cartilage (see Fig 1B). The amount of damage an ischemic stroke causes is related to the parts of the brain that are affected and depend on the stroke severity (see Fig 1C).

A



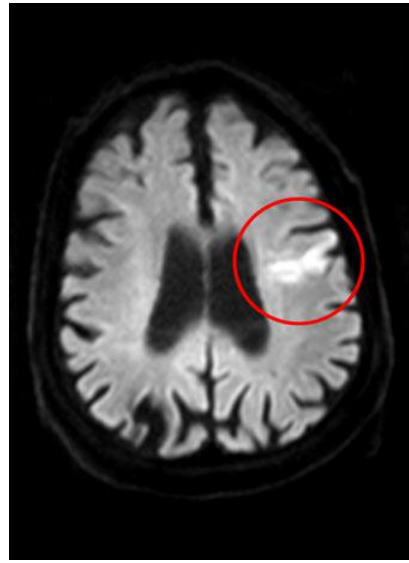
B**C**

Fig 1. Carotid stenosis and Imaging modalities of an ischemic stroke. (A) A cartoon illustrates the development of a plaque in the carotid artery. (B) The CT image reconstruction demonstrates an atherosclerotic plaque at the bifurcation of the carotid artery. (C) The MRI shows an acute ischemic stroke in the left middle cerebral artery territory (red circles). Representative radiological images are from our radiology clinic.

Once patients have been diagnosed, medications and carotid endarterectomy are the two most common treatments. Generally, medications are recommended for patients who have carotid stenosis of less than 50% or no symptoms (Hobson 2008). Because the mechanism of subtypes of stroke are distinct, the medications require different treatment strategies. For patients who have a moderate to high grade of carotid stenosis, or who have had symptoms (stroke or TIA), surgical treatment is the recommended option. Here, TIA is known as a transient ischemic attack with symptoms first appearing after a mini-stroke.

Thus, to remove the plaque completely from the carotid artery and restore blood flow, a carotid endarterectomy is especially indicated for patients who have a blockage greater than 50% with symptoms and blockage greater than 60% without symptoms. Studies have demonstrated that a carotid endarterectomy can significantly reduce the risk of stroke in symptomatic stenosis. In a randomized trial from NASCET (North American Symptomatic Carotid Endarterectomy Trial Collaborators 1991), the procedure reduced the 2-year risk from 26% to 9% and the 5-year risk from 22.2% to 15.7% in patients with 50–69% carotid stenosis. However, there is no benefit in patients with stenosis of less than 50%.

Furthermore, in asymptomatic carotid stenosis, carotid endarterectomy can also benefit by reducing the risk of stroke from 11% to 5.1%, as shown in another randomized trial (Executive Committee for the Asymptomatic Carotid Atherosclerosis

Study 1995). Finally, carotid stenting is an alternative to carotid endarterectomy, particularly in patients at high surgical risk.

1.2 Etiology and pathogenesis

1.2.1 Atherosclerosis

Within the etiology and pathophysiology of an ischemic stroke, atherosclerosis of the carotid artery is the most common disorder (Glisic 2017). Conventionally, atherosclerosis refers to a chronic progressive inflammatory disease, complicated by progressively increasing atherosclerotic plaques within the inner arteries walls. An underlying atherosclerotic plaque not only gradually narrows the lumen, but it also causes thrombotic events or emboli in relation to an acute rupture of an unstable (vulnerable) plaque (Liem 2017). Fundamentally, the whole process is a complex interaction of many factors in the immune system and environment, which contains lipid accumulation and modification, chronic inflammation, immune disorders, oxidative stress, epigenetics, and multiple risk factors (pollution, smoking, mental health, diet, and lifestyle) (Xu 2018).

Generally, a normal arterial wall contains three layers: intima, media, and adventitia. In most cases, atherosclerotic plaques are known to be initiated after a universal pathology step called adaptive intimal thickening of smooth muscle cell accumulation within the intima and an endothelial injury and dysfunction, resulting in the adhesion of blood leukocytes, lipid uptake (low density lipoproteins, LDL), the adhesion and migration of circulating monocyte, and the formation of a fatty streak (xanthoma) that macrophages phagocytose the lipid, becoming foam cells (Bentzon 2014).

Additionally, lipid pools can be observed in the intima beneath the layers of foam cells, which is termed pathological intimal thickening. Furthermore, a necrotic core is present when these aforementioned lesions grow into a confluence lesion, also known as a fibroatheroma. Concurrently, lesion progression involves the differentiation and migration of vascular smooth muscle cells from the media layer to the space between the necrotic core and lumen, as well as the generation of a SMC/collagen-rich fibrous cap (Libby 2011). With the progression of atherosclerosis, inflammation leads to hypoxia in the neo-angiogenesis in the plaque. These new vessels are fragile and prone to hemorrhage (Moulton 1999).

Subsequently, thinning of the fibrous cap – which is the gradual loss of vascular smooth muscle cells (VSMC) from fibrous caps – may cause a subsequent plaque rupture and thrombosis that obstruct the carotid artery, followed by a microcalcification as a type of healing process. Ultimately, the risk of ischemic stroke increases (Mughal 2011).

1.2.2 Vulnerable plaque and vascular smooth muscle Cell (VSMCs)

Based on morphology and histology, carotid atherosclerotic plaques can be characterized as stable or unstable (vulnerable). In 1989, Muller first described the “vulnerable plaque” concept in coronary artery stenosis (Muller 1989). The term refers to all plaques at risk for thrombosis and prone to rapid progression in becoming rupture lesions (Naghavi 2003). Although other terms such as “high-risk plaque,” unstable plaque, AHA type IV plaque, noncalcified plaque, and soft plaque have been proposed, it is still recommended to use “vulnerable plaque” as a uniform term to help standardize terminology. It has already been widely used in various reports in medical literature and was adopted by investigators and clinicians (Kolodgie 2001) (Stary 1995). Meanwhile, it seems to be the most suitable term for defining plaques susceptible to complications.

Supported by histopathology studies on the constituents of carotid artery plaques after ischemic strokes, the composition of a vulnerable plaque could determine the stability of the plaque, making it prone to rupture and eventually leading to clinical events (Redgrave 2006) (Spagnoli 2004).

According to Adamson (Adamson 2015), plaques with a thin or disrupted smooth-muscle cell-rich fibrous cap, a large number of cells positive for macrophage markers, a large volume lipid-rich necrotic core, inflammatory infiltrates, microcalcification, intraplaque hemorrhage (IPH), positive remodeling, and neo-vasculature growth are considered “vulnerable.” Figure 2 presents the composition of a vulnerable plaque in the arterial system.

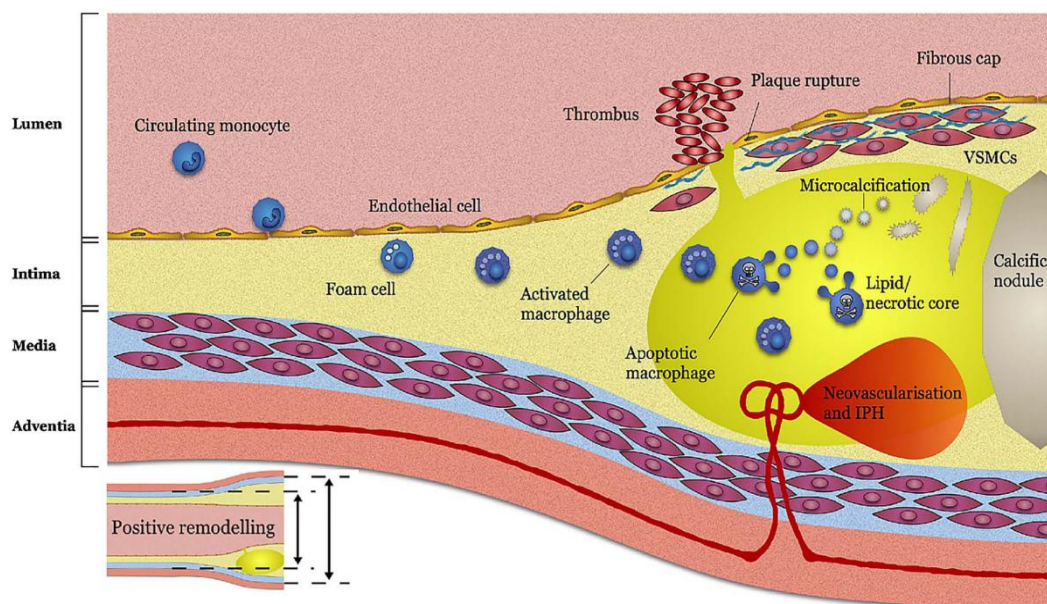


Fig 2. Figure illustrating the features of a vulnerable plaques according to (Adamson 2015). Recognized features of the vulnerable plaque include a thin SMC-rich fibrous cap, a high number of macrophages, a large necrotic core, positive remodeling, microcalcification, intraplaque hemorrhage (IPH), and neovascularization.

Thus, to understand the mechanisms leading to plaque vulnerability, great effort has been committed to recognizing the pathological features of those unstable plaques. It is not surprising that a wide array of mechanisms have thus been proposed as potential contributors to unstable carotid atheroma development and ultimately rupture, including apoptosis and insufficient proliferation of SMC, which essentially leads to vulnerability and instability of the fibrous cap, with subsequent rupture (Maegdefessel 2014).

Histologically, a thin SMC fibrous cap can play a vital role in determining plaque susceptibility, because further thromboembolic progression may eventually lead to a dramatic complication, following by a thin cap rupture (Hatsukami 2000). In the observations of animal studies and human specimens, most schemes of plaque vulnerability posit the role of VSMC due to its athero-protective properties, where less VSMCs within the fibrous cap and shoulder area plaques are more prone to rupture. In this regard, VSMCs in advanced lesions are viewed as a detrimental factor for plaque stabilization.

At our laboratory, we have focused on this VSMC behavior in atherosclerosis. Increasing evidence has indicated that the origin or modulation of VSMC can effectively impact the disease pathogenesis through these processes, such as VSMC proliferation, VSMC migration, VSMC apoptosis, VSMC senescence, and VSMC phenotypic switching (Bennett 2016). Figure 3 shows the interrelated processes that VSMCs undergo in advanced plaques.

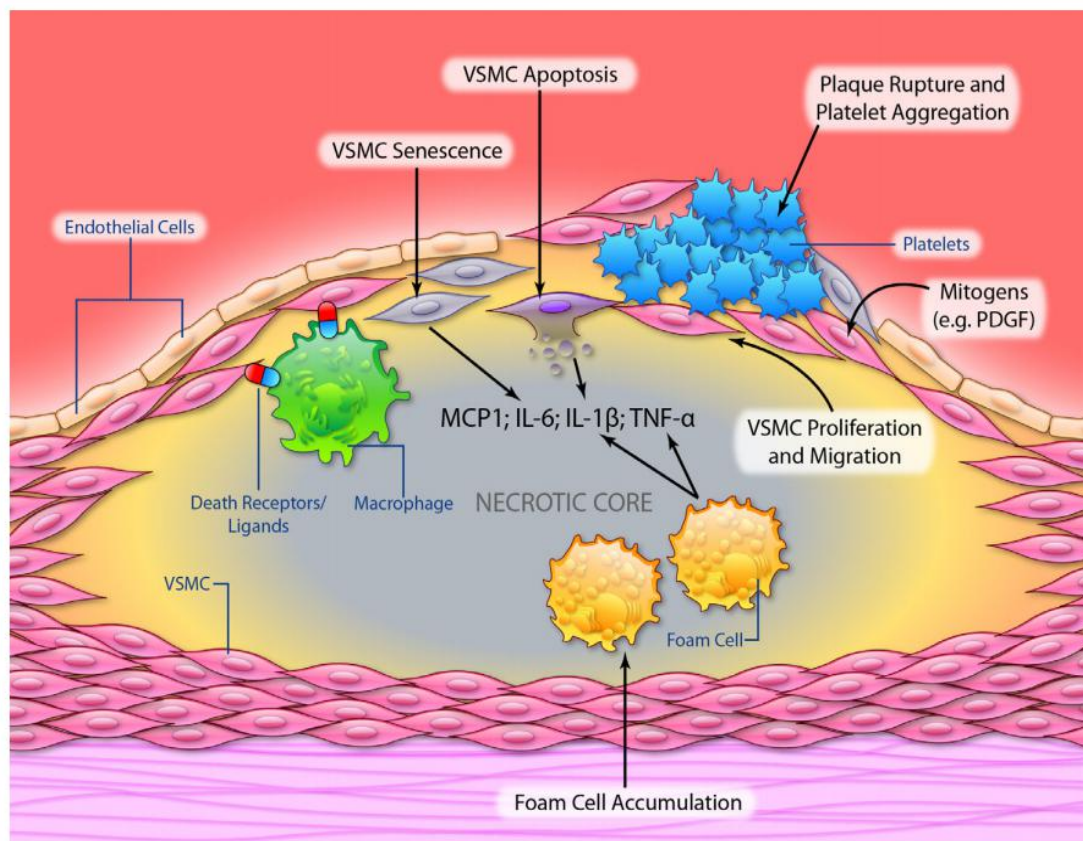


Fig 3. Illustration of processes that VSMCs undergo in vulnerable plaques (Bennett 2016). Generally, the thickness of the fibrous cap and the degree of inflammation are considered key to plaque stability. Thus, the imbalance between the proliferation and migration of VSMCs and the apoptosis and senescence of VSMCs may generate a vulnerable plaque from a stable plaque by reducing the VSMC population.

1.2.3 Phenotypic switching of VSMCs in atherosclerosis

During embryonic vasculature development, VSMCs can switch from a synthetic to a contractile phenotype. Contractile tone is maintained by highly organized contractile proteins in non-diseased vessels. However, in response to vascular injury, VSMCs can further switch back to their synthetic characteristics followed by increasing cell size in morphology, increasing rates of cell proliferation, migration, and extensive extracellular matrix (ECM) synthesis (Alexander 2012). As such, this ability termed phenotypic switching has long been considered important to atherosclerosis. The scheme below provides an overview of vascular remodeling in atherosclerosis (see Fig 4).

Today's debate on the phenotypic switching of VSMCs is focused around the identification of VSMCs /Macrophages within lesions and the effects of different origins of VSMCs in atherosclerosis. Although these VSMC-derived macrophage-like cells within advanced lesions have long been considered as pro-atherogenic, current research has determined that phenotypic switching might also play a beneficial role in the maintenance of plaque stability. Compelling evidence has shown that VSMC phenotypic switching or transformation within advanced atherosclerotic plaque is KLF4 dependent, and the selective loss of KLF4 within VSMCs can reduce lesion size, increase fibrous cap thickness, result in the loss of VSMC-derived macrophage-like cells, and increase VSMC-derived cells that contribute to plaque stabilization within the fibrous cap (Shankman 2015). Additionally, studies have demonstrated that VSMC-derived macrophage-like cells can reduce phagocytosis and directly promote necrotic core progression within advanced lesions (Schrijvers 2005) (Vengrenyuk 2015). Thus, VSMC behavior in atherosclerosis is remarkably critical, but the consequences of phenotypic switching by VSMCs may vary throughout atherosclerosis.

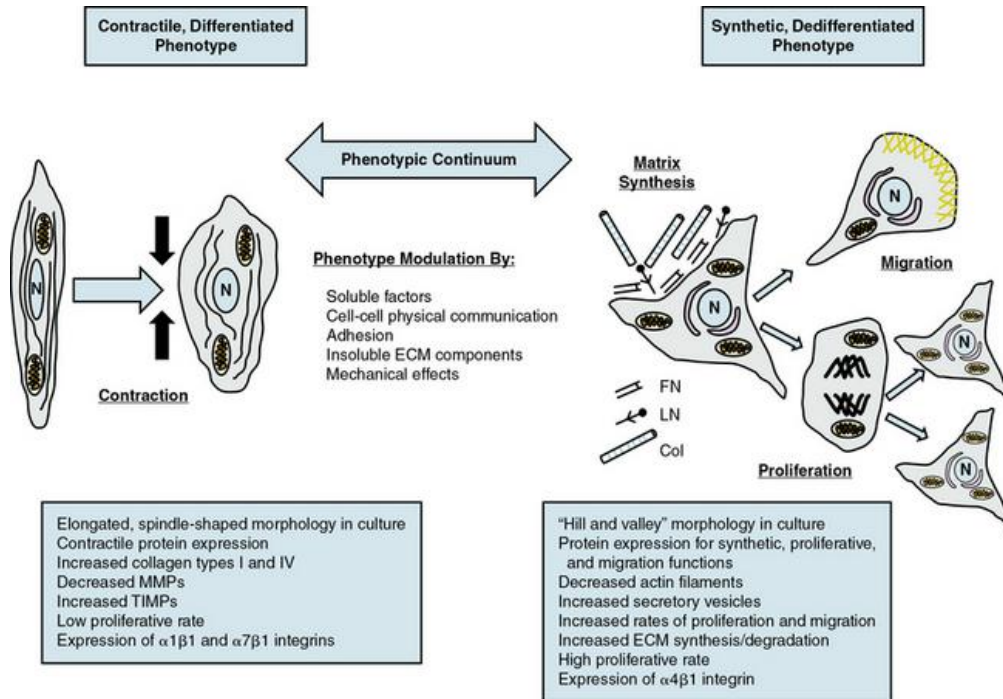


Figure 4: Schematic summarization of the phenotypic switching of VSMCs (Beamish 2010). The characteristics of VSMC contractile, differentiated, or “quiescent” phenotype are on the left, and VSMC synthetic, dedifferentiated phenotype on the right. ECM, extracellular matrix; FN, fibronectin; LN, laminin; Col, collagen; MMPs, matrix metalloproteinases; TIMPs, tissue inhibitors of MMPs.

1.3 CHI3L1/YKL-40

1.3.1 CHI3L1 in preliminary differential Transcriptome array analysis

In an effort to explore the novel molecular mechanisms involved in carotid plaque vulnerability, we have used the GeneChip 2.0 Human Transcriptome Array to profile the plaque fibrous caps, which were isolated by laser-capture microdissection (LCM) from a total of 40 age-, gender- and medication-matched patients undergoing carotid endarterectomy in our department of Vascular and Endovascular Surgery at the Klinikum rechts der Isar of the Technical University Munich (TUM; 20 patients with ruptured plaques and symptoms within the last 7 days vs. 20 samples from asymptomatic patients with histologically-defined stable lesions; Figure 4).

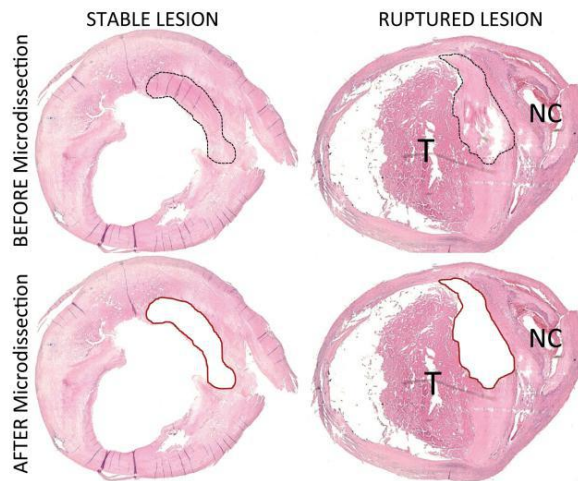


Figure 4: Stable and ruptured carotid artery lesions before and after laser-capture microdissection (LCM) of fibrous caps. Consecutive sections of patients were pooled to achieve high enough yields of RNA for analysis (50ng of total RNA were required). NC=necrotic core; T=thrombus.

The tissue was provided through the Munich Vascular Biobank, one of the largest human vascular biobanks containing more than 2700 vascular tissue and plasma samples, along with clinical data obtained from patients undergoing surgery in our Department of Vascular and Endovascular Surgery. Thus, based on a preliminary data analysis, one of the most intriguing targets we identified as being substantially increased (8.6-fold up-regulation) in ruptured versus stable lesions is Chitinase-3-like-protein-1 (CHI3L1, also known as YKL-40) (Fig 5). Additionally, a recently published study from the BiKE cohort (Biobank of Karolinska Endarterectomies) from Stockholm, Sweden, confirmed our results for CHI3L1 up-regulation in plaque specimens from symptomatic, rather than asymptomatic, patients with advanced carotid atherosclerosis and subsequent stroke (Perisic 2016).

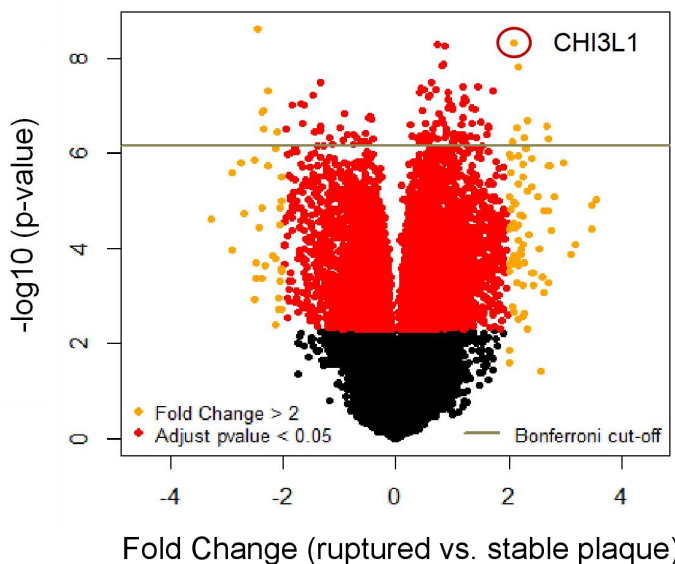


Figure 5: The identification of DEGs (differentially expressed genes). In the volcano plot, orange dots represent the fold change of DEGs between the rupture and stable groups greater than 2. CHI3L1 was detected as the most upregulated.

1.3.2 CHI3L1 in Identification and characterization

Family 18 chitinases are an ancient gene family, including the true chitinase, acidic mammalian chitinase (AMCase) and the chitinase-like proteins (CLP) that lack chitinase activity as a result of mutations in their highly conserved putative enzyme sites (Bleau 1999). Chitinase-3-like-1 (CHI3L1) is also known as YKL-40 in humans and as the homolog breast regression protein-39 (BRP-39) in mice. Additionally, its porcine homolog 38-kDa heparin-binding glycoprotein (GP38K) is the prototype of this subfamily. First, CLP GP38K was discovered in swine vascular smooth muscle cells (Millis 1985); subsequently, a variety of homologs with different names, including human HcGP-39, bovine 39-kDa whey protein, and *Drosophila* imaginal disc growth factors, have been described by researchers (Lee 2011). It was not until 1992 that CHI3L1 was first identified in the medium of a human osteosarcoma cell line MG-63 (Johansen 1992).

1.3.3 CHI3L1 in Biology and physiology

CHI3L1 is a 40-kDa heparin-, chitin- and collagen-binding glycoprotein encoded by the CHI3L1 gene on chromosome 1 (Rathcke 2009). It is expressed in a variety of cells, including VSMCs, macrophages, neutrophils, fibroblasts, hepatic stellate cells, colonic, ductal, airway epithelial cells involved in tissue inflammation, chondrocytes, and synovial cells involved in human connective tissue cells and cancer cells (Johansen 2006). Additionally, studies have increasingly indicated that CHI3L1 is associated with both acute and chronic inflammation and many human cancer malignant processes, where it mediates cell proliferation, cell migration, cell differentiation, cell apoptosis, angiogenesis, and tissue remodeling (Chen 2017).

For example, researchers found that CHI3L1 produced by activated macrophages can induce the maturation of monocytes to macrophages during the late stages of differentiation. Therefore, it is regarded as a differentiation marker in macrophages (Rehli 2003). Additionally, according to Nishikawa (Nishikawa 2003), CHI3L1 expression by differentiated VSMCs is also an adhesion and migration factor in vitro, suggesting an important role in angiogenesis. Meanwhile, another in vitro study identified that CHI3L1 can stimulate cell proliferation in a dose-dependent manner in human connective tissue cells (Recklies 2005). Furthermore, observations in mice have demonstrated that CHI3L1 has a critical role in protection against inflammatory apoptosis as an important regulator of Th2 cytokine effector (Lee 2009). It may also inhibit the toxic effects of hyperoxia, making it a vital regulator of oxidant injury and epithelial apoptosis in the murine and human lung (Sohn 2009). In a study regarding glioblastoma (the most lethal primary brain tumor), Shao et al (Shao2014) found that CHI3L1 can increase tumor angiogenesis in mural cell-associated vessel diameter, density, and stability, and decrease the angiogenesis in vessel permeability. So far, according to Di Rosa (Di Rosa 2016), Figure 5 summarizes the current CHI3L1 biological activities.

1.3.4 CHI3L1 in atherosclerosis

As high levels of serum CHI3L1 is a biomarker of poor prognosis in patients with cancer, inflammation, and increased tissue remodeling (Roslind 2009), more clinical studies have described elevated CHI3L1 levels as independently associated with the presence and mortality of CVD (Kastrup 2009). In patients who are suffering myocardial infarction (MI), higher CHI3L1 levels were found in thrombolized patients than non-thrombolized patients (Nojgaard 2008). Additionally, earlier pathology studies have also revealed that there are high levels of serum CHI3L1 existing in carotid atherosclerosis, without explaining or exploring the vascular biology behind this elevation (Michelsen 2010).

Furthermore, recent clinical studies found a positive correlation between CHI3L1 levels and stroke. Studied in the general population, elevated CHI3L1 values indicated an increased risk of ischemic cerebrovascular events. An increased expression of CHI3L1 in the CSF of patients with acute ischemic stroke is correlated with clinical stroke severity (Kjaergaard 2010). Bonneh-Barkay reported that CHI3L1 was induced in astrocytes in all kinds of neurological diseases, such as stroke, and that it was mostly associated with astrocytes residing around inflammatory cells (Bonneh-Barkay 2010). Moreover, Chen' research showed that elevated CHI3L1 is a significant and independent biomarker to predict poor clinical outcomes in 141 patients with large-artery atherosclerosis (LAA) stroke (Chen 2017).

Interestingly, baseline-elevated plasma CHI3L1 levels have been shown to be associated with the development of ischemic stroke, but not with MI (Park 2012). This discrepancy is possibly explained by differences in the pathogenesis of atherosclerosis in carotid and coronary vasculature and might also be related to differences in levels of lipids and lipoproteins. It is also possible that elevated CHI3L1 is a direct cause of ischemic stroke but not of MI. A Mendelian randomization study on this regard, using genetic variants, was able to show that lifelong elevated CHI3L1 levels are largely un-confounded and not prone to reverse causation (Kjaergaard 2010). It is partly heritable, and rs4950928, a single nucleotide polymorphism in the proximal promoter of CHI3L1, accounts for an estimated 9% of its variance (Kjaergaard 2016). Mechanistically, c-myc/myc-associated factor X transcriptional factors bind well to the major allele of rs4950928, which increases CHI3L1 transcription and consequently elevates YKL-40 levels.

Although its biological mechanism and role in plaque vulnerability and VSMC survival have yet to be identified, to date, studies have demonstrated that CHI3L1 can be regulated by various cytokines and hormones. For example, inflammatory cytokines like tumour necrosis factor alpha (TNF- α) and interleukin 1 beta (IL-1 β) can stimulate the expression of CHI3L1 through the sustained activation of NK-kappa B, in particular in chondrocytes. (Ling 2004). Additionally, published data investigating pulmonary hypertension indicated that CHI3L1 might influence SMC proliferation and migration through protease activated receptor type 2 (PAR-2)-,

AKT-, ERK-, and p38-dependent mechanisms (Bara 2012). Other studies have previously shown that fibroblast migration is not affected by CHI3L1 (Catalan 2012). However, active crosstalk between macrophages, neutrophils, and fibroblasts is known to regulate extracellular matrix deposition (Rudolph 2010). Therefore, apart from fibrous cap enriched SMCs, fibroblasts might be modulated in response to CHI3L1 elevation. Thus, further efforts should be conducted studying the mechanisms that contribute to plaque instability. In fact, cellular receptors that regulate the biological effects of CHI3L1 have not been identified, and so far, only a potential network involving the CHI3L1 and Toll Like Receptor 4-signaling pathway has been published (Kamba 2013) (Fig 5).

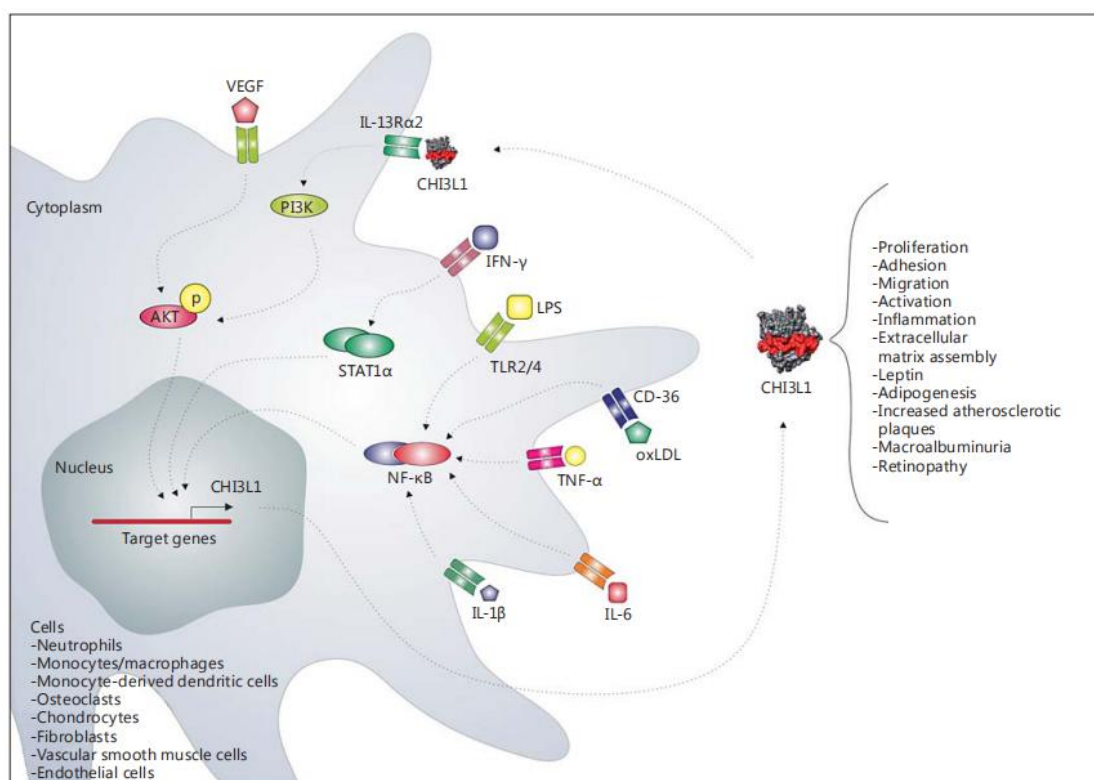


Figure 5: CHI3L1 biological activities and molecular network (Di Rosa 2016).

CHI3L1 can be expressed by types of cells. Through the mediator PI3K followed by the phosphorylation of AKT, CHI3L1 can be transcribed and further regulated in many biological processes, such as cell proliferation, cell adhesion, cell migration, activation, inflammation, and even increased atherosclerotic plaques. During the activation of CHI3L1, the inflammatory cytokines IL-6, TNF- α and IL-1 β or inflammation mediators oxLDL can increase CHI3L1 expression by the continued activation of NF-kappa B, which in turn enhances the expression of CHI3L1.

1.3.5 Main aims of the doctoral thesis

Extraordinary efforts have been devoted to determining the pathophysiological and molecular characteristics of the diseased plaques and the surrounding vasculature, with the goal of developing novel diagnostic and therapeutic strategies to prevent vulnerable plaque rupture. Thus, the study presented in this thesis was designed to

explore the functional role of CHI3L1 and the mechanism behind atherosclerotic plaque vulnerability *in vitro*, and there are two main goals of this doctoral thesis, introduced below:

Aim 1: Exploring the functional role of CHI3L1 in atherosclerotic plaque vulnerability *in vitro*.

Hypothesis 1.1: CHI3L1 plays a role in VSMCs cell fate *in vitro*.

Hypothesis 1.2: CHI3L1 plays a role in VSMCs phenotypic switching *in vitro*.

Aim2: Defining the mechanism behind how CHI3L1 modulation effects cell fate decisions in VSMCs.

Hypothesis 2.1: Define the cellular mechanism of CHI3L1 biological activities in VSMCs cell survival.

Hypothesis 2.2: Define the cellular mechanism of CHI3L1's biological activities in VSMC phenotypic switching.

To test this hypothesis, a set of experiments have been carried out in our Vascular Biology lab at the TUM. However, we have analyzed human stable and vulnerable plaques with immunohistochemistry, performed live-cell imaging analysis in primary patient-derived VSMCs with CHI3L1 modulation, implemented TaqMan gene expression array, and used bioinformatic tools to predict the potential interacting network. The relative details are explained in the methods and results chapters below.

2. MATERIALS AND METHODS

2.1 Munich Vascular Biobank and cell culture

2.1.1 Munich Vascular biobank

The Munich Vascular Biobank (MVB) is one of the largest human vascular biobanks, collecting more than 2700 vascular tissues and over 4400 serum from patients undergoing surgery in our Department of Vascular and Endovascular Surgery (from January 2004 to December 2018). We summarize the details in Table 1. Permission to collect human biospecimens was granted by the Ethics Committee of our local Hospital (Klinikum rechts der Isar, Munich, Germany). Written consent was obtained from all patients.

Table 1. List of biospecimens collected over the years.

Year	*CAROTID	AAA	PAD	FFPE	Serum
	*FFPE	Serum	FFPE		
2004	79	47			
2005	72	63	8	17	
2006	36	84	36	84	
2007	79	56	40	89	

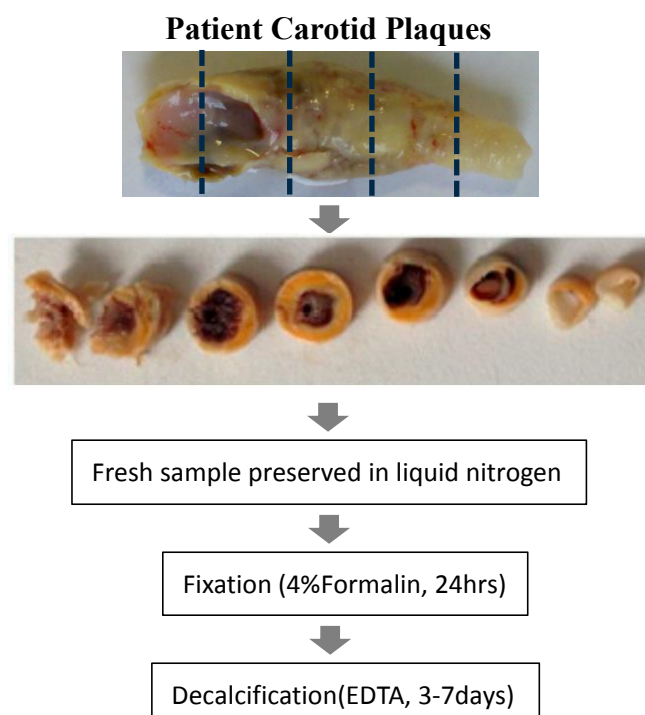
2008	63	72	34	84		
2009	100	62	40	60	63	90
2010	94	58	40	72	77	78
2011	121	87	38	91	51	133
2012	122	111	33	136	62	251
2013	126	99	41	114	63	228
2014	92	97	24	131	63	259
2015	126	131	26	126	84	294
2016	124	117	30	124	142	228
2017	173	156	48	127	60	116
2018	160	154	43	125	38	25
*Total:	1567	1394	481	1380	703	1702

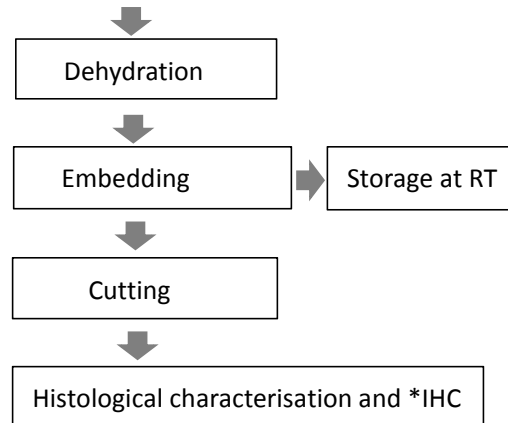
*carotid plaques, n=1567; abdominal aortic aneurysm, n=481; peripheral arterial disease, n=703, including peripheral aneurysms and thrombus. FFPE: formalin fixed paraffin embedded. (For this table data from our publication data: Pelisek 2019).

2.1.2 Carotid artery tissue processing

Following surgical excision of an atherosclerotic plaque, the tissue was delivered contemporary to the lab for further processing. There, the plaque was segmented in blocks of 3–4 mm and immediately frozen in liquid nitrogen for further molecular analysis. The remaining segments were fixed in 4% formalin, followed by dehydration and embedding in paraffin. An example of our carotid tissue processing is shown in Figure 6.

Fig 6: Schematic chart of our patient carotid tissue processing.





*IHC: immunohistochemistry; RT: room temperature. (For this chart from our publication data: Pelisek 2019).

2.1.3 Isolation of primary patient-derived vascular smooth muscle cells

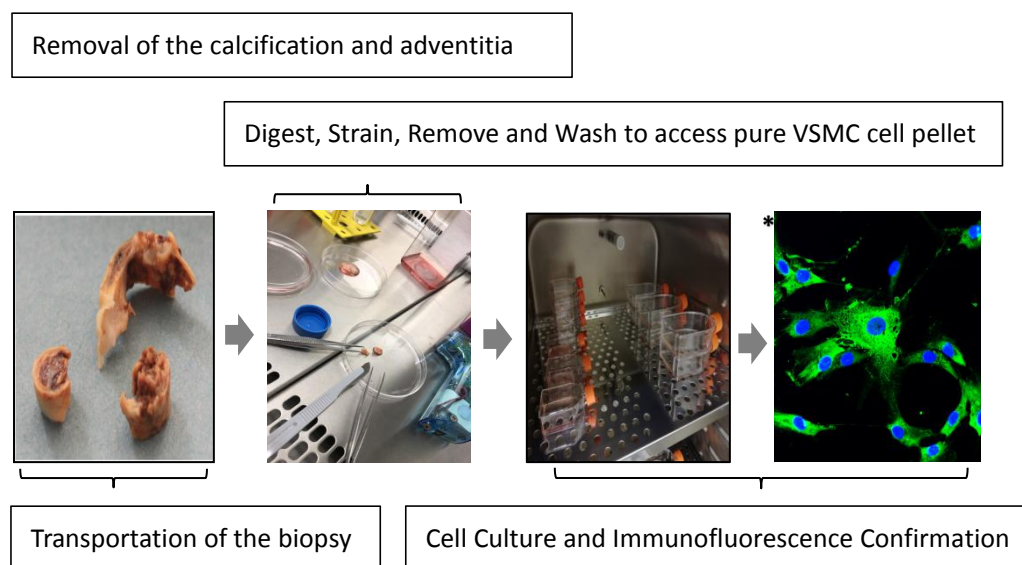
Primary patient-derived VSMCs were isolated from patients’ carotid atherosclerosis plaques. The tissue we investigated – along with clinical feature data from each patient – were all provided by the Munich Vascular Cell Biobank (see Table 2). We selected three patient samples with similar clinical characteristics and comparable pathological features.

Table 2. Information on patients of carotid biosies.

Biopsy name	Age	Sex	Disease location	Stenosis degree [%]
G183/18	75	Male	carotis interna	70
G216/18	74	Male	carotis interna	80
G224/18	74	Male	carotis interna	80

Briefly, following surgical excision, the patients’ carotid biopsies were transported from the operation room to the lab in DMEM/F-12 medium (Sigma-Aldrich, St. Louis, MO). After removal of the adventitia, the pure VSMC bundles were isolated from the media of the vessel. The specimens were then cut into small pieces by removing the calcifications to aid digestion by Collagenase A (Roche, Mannheim, Germany), then placed inside the incubator at 37°C for 4-6 hours. The cells were then strained using a 100µm sterile cell strainer (Corning, Durham, USA) to remove debris. The cell suspension was centrifuged (400 g/5 min). Then, the cells were suspended with 15 ml of DMEM/F-12. This process was repeated twice, and the cells were transferred into a T-25 Flask (Corning, Oneota, USA). Growth medium was first changed after 72 hours and then regularly every 48–72 hrs. Furthermore, smooth muscle cell marker SM22-alpha (Abcam, Cambridge MA, USA) expression was analyzed by immunofluorescence (Leica, Munich, Germany). An example of the cell isolation is shown in Figure 7 below.

Fig 7: Schematic chart of primary patient-derived VSMCs isolation.



*Immunofluorescence demonstrates the primary patient-derived VSMCs expression of adult smooth muscle cell marker SM22 alpha.

2.1.4 Culture of Primary Patient-Derived VSMCs

Primary patient-derived VSMCs were cultured in SMC growth medium (PeloBiotech, Martinsried, Germany) supplemented with SMC growth supplement classic (PeloBiotech, Martinsried, Germany). Cells were cultivated in plastic culture flasks (25/75cm²), 6-well plates, 24-well plates, 96-well plates (BD Bioscience, Heidelberg, Germany) depending on the experiments intended and incubated in a 5% CO₂ atmosphere at 37°C. After cells were grown to 70%-80% confluence, passage 4-6 were used for all further experiments. For incubation in the IncuCyte ZOOM, the same medium was used and changed every 3 days.

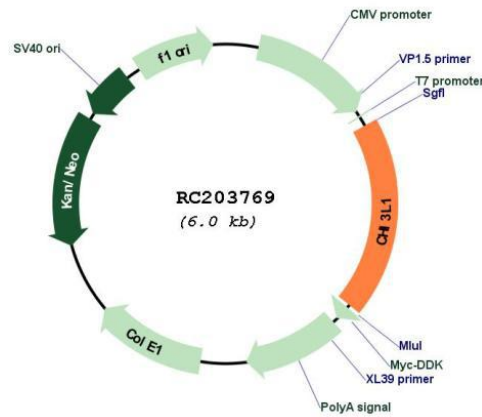
2.1.5 CHI3L1 Recombinant plasmid

Today, plasmids most commonly used in the field of recombinant DNA technology have become an essential tool in molecular biology. Within a cell that can replicate independently, plasmids are small, circular, double-stranded DNA molecules and they serve as vectors to amplify genetic information in foreign hosts. For overexpressing an interest gene, plasmid DNA is referred to as cloned DNA, and this process of generating multiple identical copies of a recombinant DNA molecule is known as DNA cloning. Additionally, these recombinant plasmids are derived from mRNA and including 5' and 3'UTRs. In this study, our recombinant plasmid DNA (pCMV6-CHI3L1) and the pCMV6 empty vector used for negative control were all purchased from OriGene Technologies (Rockville, MD). It is Kanamycin resistant, and its plasmid map and cloning scheme are shown in Fig 8.

To produce stable quality and large quantities of DNA for further transfection

experiments, we first transformed both plasmids into competent cells and generated a glycerol stock. Later, following the manufacturer's protocol, cells were transfected at concentrations of 5, 50, and 500 ng/ μ L with a lipofectamin 3000 transfection kit (Invitrogen, Carlsbad, CA). Further, the treated cells were examined for cell proliferation, migration, and apoptosis by using IncuCyte system and VSMC phenotypic switching was investigated by using qPCR.

A



B

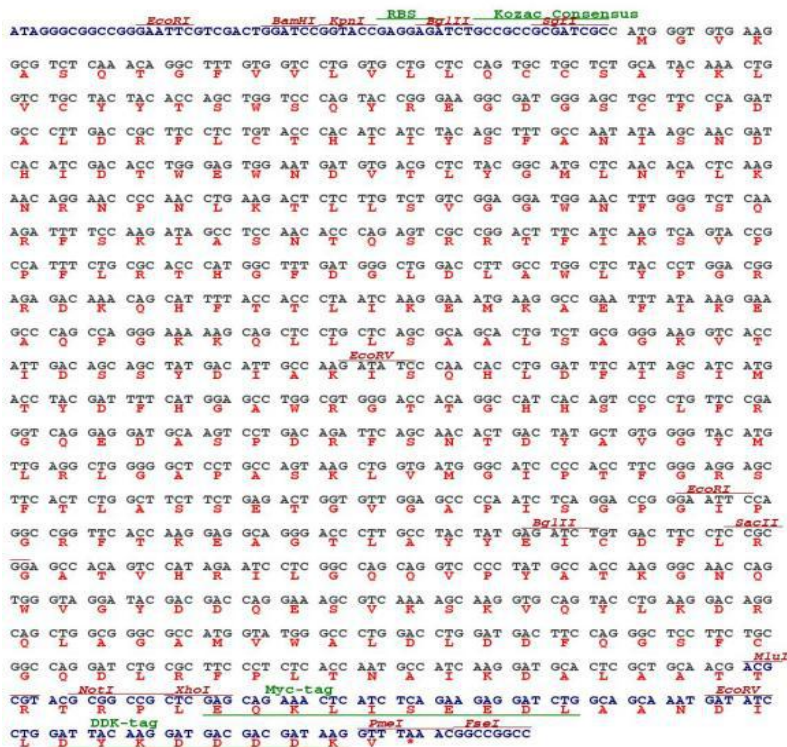


Fig 8. CHI3L1 Expression Plasmids. (A) Plasmid circular map for CHI3L1. (B) Cloning scheme for CHI3L1.

2.1.6 CHI3L1 Knockdown

Functional analysis by mRNA knockdown using siRNA (small interfering RNA) is now routine in science research; RNA interference (RNAi) can be triggered by siRNAs that cause strong, yet transient, inhibition of gene expression on specific genes. These siRNAs can be synthesized and transfected into mammalian cells, resulting in effective suppression of gene expression. Our CHI3L1-specific human 27mer small interfering RNA (siRNA) oligo duplex and a universal negative scramble control duplex was all purchased from OriGene Technologies (Rockville, MD). The following three unique oligonucleotides (siCHI3L1) were synthesized, as shown in Table 3.

Duplexes are stored in a 20 μ M final concentration at -20 $^{\circ}$ C. After transfection, RNA is harvested from the transfected cells and used in quantitative RT-PCR to verify the loss of gene expression. Then, the most efficient siCHI3L1 duplex are directly used for transfection and gene-knockdown studies after the validation of efficiency. Cells were transfected at different amounts of 10, 30, and 60 pmol of siRNA (10 μ M) by using RNAiMAX reagent (Invitrogen, Carlsbad, CA). Furthermore, we examined the gene-knockdown in cell proliferation, migration, and apoptosis by using the IncuCyte system and investigated VSMC phenotypic switching by using qRT-PCR.

Table 3. Duplex sequences of three unique siCHI3L1.

Name of siRNA	Duplex sequences
SR319700A	rArUrCrArArGrUrCrArGrUrArCrCrGrCrCrArUrUrUrCrUGC
SR319700B	rCrArUrUrGrCrCrArArGrArUrArUrCrCrCrArArCrArCrCTG
SR319700C	rArArGrCrCrCrArGrCrUrUrGrArArArCrCrUrUrCrArCrUrUTA

2.2 RNA isolation and qRT-PCR

Cells were harvested at 24 and 48 hours after transfection. Total cellular RNA was isolated with the RNeasy Plus Mini Kit (Qiagen, Hilden, Germany) following the manufacturer's protocol. The RNA concentration was measured by Nanodrop (Thermo Fisher Scientific, Munich, Germany), and cDNA was synthesized with the High Capacity RNA-to-cDNA Kit (Thermo Fisher, Vilnius, Lithuania). For each assay, 4 μ l DNA was added into a 20 μ l reaction volume, including 1 μ l the 20x TaqMan Assay, 10 μ l TaqMan Master Mix (Life Technologies, Austin, TX), and 5 μ l Nuclease-Free Water. The reaction was performed using the StepOnePlus Real-Time PCR System (Life Technologies, Singapore) with the following cycling conditions (Table 4). For each real-time PCR amplification, measurements were performed in triplicate. Quantification was normalized to housekeeping control RPLP within the

log-linear phase of the amplification curve obtained for each primer set using the $\Delta\Delta$ CT method and presented as a fold induction with mean standard deviation.

Step	Temperature	Time (standard cycling model)	Cycles
UNG incubation*	50°C	2 minutes	1
Enzyme activation	95°C	20 seconds	1
Denature	95°C	1 seconds	40
Anneal/Extend	60°C	20 seconds	40

Table 4. Duplex sequences of three unique siCHI3L1. *Carryover amplicons result in false-positive amplification during PCR. Uracil-N- Glycosylasecan is used to degrade many contaminating carryover amplicons.

2.3 Immunohistochemistry

Atherosclerotic plaque for immunohistological staining was performed on 2.5 μ m thin slices of tissue fixed with formaldehyde and embedded in paraffin (FFPE). Following the instructions of the manufacturer, procedures were carried out with the Dako Real Detection System Peroxidase/DAB kit (Dako, Glostrup, Denmark). To compare the distribution of CHI3L1-positive cells, VSMCs, and macrophages in ruptured and stable plaques, antibodies were diluted in the antibody diluent also obtained from Dako and used at optimal dilutions, as shown in Table 5. Images were captured and analyzed using a Leica DFC310 FX inverted fluorescent microscope (Leica, Munich, Germany) and scanned with a PerciPoint Digital microscope system (Perci, Freising, Germany).

Table 5. Antibodies used for IHC.

Ab Name	React with	Clone	Brand&Cat. Nr.	Dilution	Counterstained with Hematoxylin
CHI3L1	Human	Rabbit	Abcam (ab180569)	1:50	30s
SMC- α	Human	Mouse	Abcam (ab7817)	1:200	20s
CD68	Human	Mouse	Dako (M0814)	1:1000	30s
Ki67	Human	Mouse	VWR	1:75	60s

			(9252-M05)		
Caspase-3	Human	Mouse	EMD (MAB10753)	1:100	60s

2.4 Live-cell imaging and analysis

2.4.1 IncuCyte Live-Cell Analysis System and IncuCyte ZOOM software

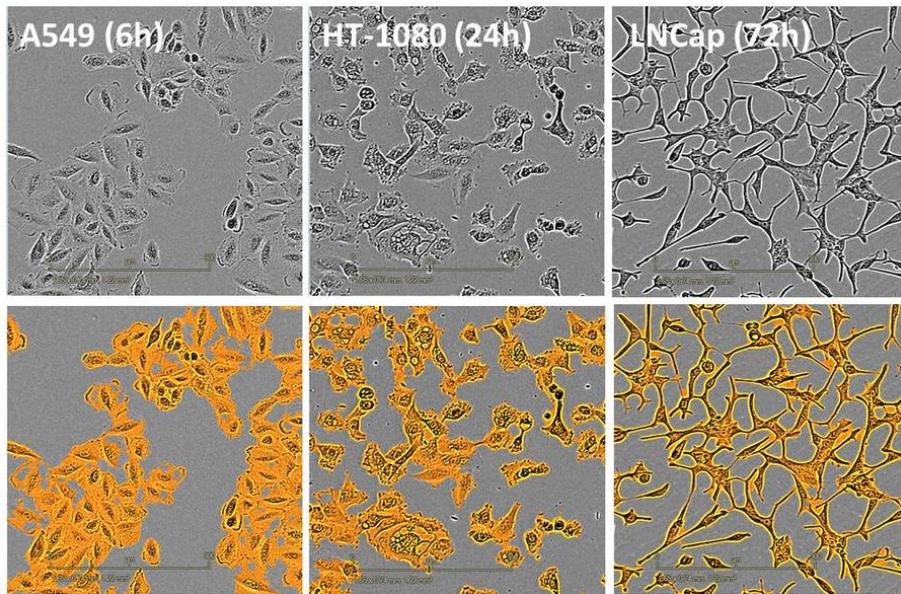
The IncuCyte live-cell analysis system (Essen Bioscience, Michigan, USA) is a real-time quantitative platform that gathers cell images (phase contrast or fluorescence) from assay microplates automatically, repeatedly within a standard incubator (Thermo GmbH, Langenselbold, Germany) (Fig9 A). The system has the unique ability to analyze different cell types and multiple applications including cell proliferation, apoptosis, migration, chemotaxis, and phagocytosis. A specialized microscope and live-cell imaging device allows researchers to make time-lapsed measurements; in each case, the full time-course data and “mini movies” of the analysis can be obtained, thus providing greater biological insight into active processes in real time. Furthermore, the IncuCyte ZOOM software provides a powerful workflow for acquiring, viewing, and analyzing images of living cells, which can help us to simplify the complex ones.

In summary, it is a widely used technology, and according to data from IncuCyte official website (www.essenbioscience.com/en/resources/publication-list), the reference number of the IncuCyte technology is over 2,000. Here, we display examples of IncuCyte application according to official data (www.essenbioscience.com/en/resources/image-gallery/) (see Fig9 B-D).

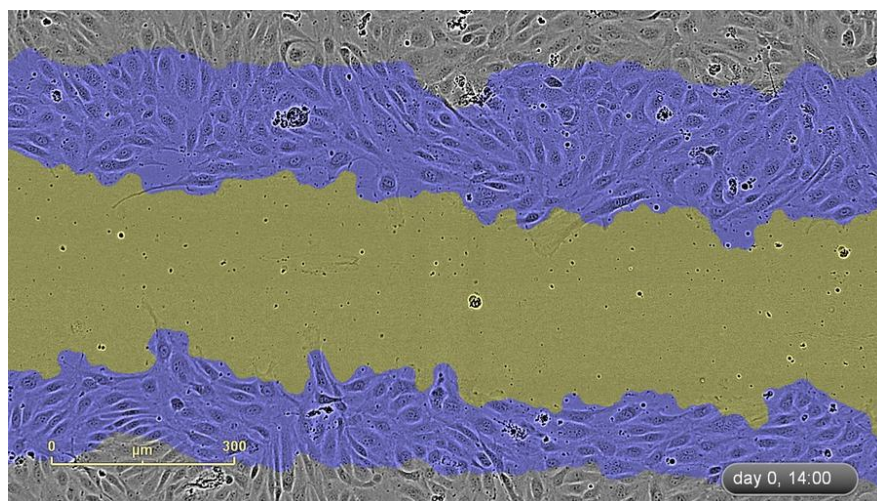
A



B



C



D

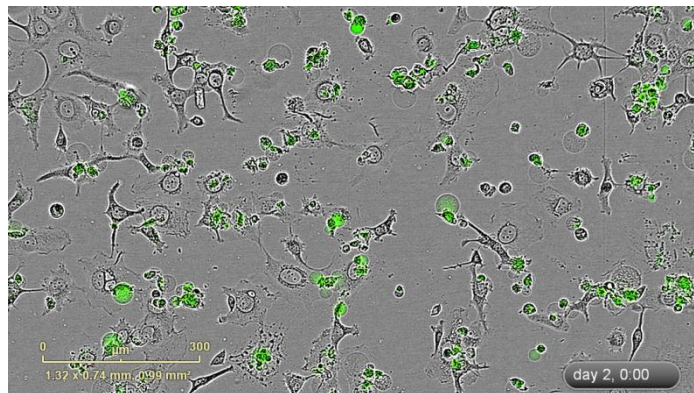


Fig 9. IncuCyte System and Different application examples. (A) IncuCyte system and a standard incubator housing the system. (B) An example of a cell proliferation measurement

according to IncuCyte official data: Phase-contrast images (10x) of A549 human lung carcinoma, HT-1080 human fibrosarcoma, and LNCap cells (androgen-sensitive human prostate adenocarcinoma cells) shown with and without the confluence mask overlaid in orange. (C) An example of a cell migration measurement according to IncuCyte official data: Phase-contrast image (10x) at 14 hours post wounding of migrating HUVECs. The initial wound is overlaid (blue areas) and the wound mask at the 14-hour point is shown in yellow. (D) An example of a cell apoptosis measurement according to IncuCyte official data: Phase-contrast and green-fluorescence blended images (10x) of HT-1080 cells in the presence of Caspase-3/7 reagent.

2.4.2 IncuCyte Scratch Wound Assay

Measurements of migration into a wound region can be carried out by the IncuCyte Scratch Wound Assay in the system (Essen Bioscience, Michigan, USA). Following the recommended protocol, cells were seeded at a density of 10,000 cells/well into 96-well Image Lock plates (Essen Bioscience, Michigan, USA), then placed into a 37°C incubator overnight. By utilizing the IncuCyte Wound Maker tool (Essen Bioscience, Michigan, USA), which is a 96-pin device designed to create homogeneous scratch wounds, uniform cell-free zones in a 96-well plate were created in the next day. After wounding, the media was immediately aspirated from each well and the cells were carefully washed twice with Dulbecco's Phosphate Buffered Saline (dPBS) (Sigma-Aldrich, St. Louis, MO). Then, transfections with expression plasmid and siRNA (as described above) were performed, using empty vector or scramble control for negative control. Time lapse images were collected at 10x magnification every half hour for a total of 48 hours. By generating masks of the wound area and measuring relative wound density, phase-contrast images of cell migration into the wounded area were automatically analyzed by the IncuCyte ZOOM software. Results were reported as the mean of three replicates±SD.

2.4.3 IncuCyte Apoptosis assay

By reading IncuCyte Caspase 3/7 green reagents (Essen Bioscience, Michigan, USA), the IncuCyte Apoptosis Assay module (Essen Bioscience, Michigan, USA) was used to detect apoptosis in real time. Under a manufacturer's protocol, we seeded our cells (100 ul/well) into a 96-well plate at a density of 3000 cells/well, that by the next day the cell confluence is approximately 30%. Then the plate was placed into the incubator overnight. Dilute apoptosis reagents 1:1000 were used in our SMCs growth medium (PeloBiotech, Martinsried, Germany) and aspirate off medium. Then, transfections with plasmid and siRNA were performed, and controls were added to the wells as well (as described above). Apoptosis was quantified as the number of green fluorescent caspase-3/7 active objects at 10x magnification alongside cell proliferation in phase-contrast cell count hourly for a total of 72 hours. Results were showed both for caspase activity and the proliferation for each individual well at each time point.

2.4.4 IncuCyte proliferation assay

Multiplexed measurements of proliferation can be combined using the IncuCyte Live-Cell Analysis System (Essen Bioscience, Michigan, USA) alongside apoptosis within the same well. According to manufacturer's protocol, we seeded our cells into a 96-well plate (Corning, Durham, USA) at density of 3000 cells/well. Transfections with expression plasmid and siRNA (as described above) were performed after 12 hours, using empty vector or scramble control for negative control. The experiment was conducted over a total of 72 hours, taking images repetitively at 10x magnification every hour. Analysis was quantified with the IncuCyte ZOOM software. Proliferation was monitored by analyzing the occupied area (% confluence) of cell images over time.

2.5 Prediction of potential mediators of CHI3L1 modulation

Understanding the molecular mechanism of a gene largely relies on the identification of its target genes. This demand has been addressed by the application of a combination of experimental and computational processes. To further identify a potential pathway of CHI3L1 regulation in VSMC survival, its downstream targets and phenotypic switching associated genes were predicted by using RegRNA2.0 (<http://regrna2.mbc.nctu.edu.tw/detection.html>), which is an integrated web server for identifying functional RNA motifs in an input RNA sequence. This widely used tool also successfully helped us find a transcription factor in the previous H19 project (Li 2018). Based on the mRNA of CHI3L1 and functional RNA motifs interaction, those predictions are computing binding free energy, which is a well-established statistical mechanics theory of molecular association. The input mRNA sequence of CHI3L1 in FASTA format was obtained from the NCBI Nucleotide database (NM_001276.3) and is shown below (see Table 6).

Table 6. The input mRNA sequence for relative mediators' prediction

>NM_001276.3 Homo sapiens chitinase 3 like 1 (CHI3L1), mRNA
CACATAGCTCAGTCCCAATAAAAGGGCTGGTTTGCCGCGTCGGGGAGTGGAGTGGGACAGGTATATAAAGGAAGTACAGGGCCTGGGGGAAGA
GGCCCTGTCTAGGTAGCTGGCACCAGGAGCCGTGGGCAAGGGAAGAGGCCACACCCTGCCCTGCTCTGCTGCAGCCAGAATGGGTGTGAAGG
CGTCTCAAACAGGCTTTGTGGTCCTGGTGTGCTCCAGTGTGCTCTGCATACAACTGGTCTGCTACTACACCAGCTGGTCCCAGTACCGGGGA
AGGCGATGGGAGCTGCTTCCCAGATGCCCTTGACCGCTTCTCTGTACCCACATCATCTACAGCTTTGCCAATAAAGCAACGATCACATCGAC
ACCTGGGAGTGGAAATGATGTGACGCTTACGGCATGCTCAACACACTCAAGAACAGGAACCCCAACCTGAAGACTCTCTTGCTGTGGAGGA
TGGAACCTTTGGGTCTCAAAGATTTTCCAAGATAGCCTCCAACACCCAGAGTCGCCGGACTTTCATCAAGTCAGTACCGCCATTCTGCGCACCC
ATGGCTTTGATGGGCTGGACCTTGCTGGCTTACCCTGGACGGAGAGACAAACAGCATTACCACCCTAATCAAGGAAATGAAGGCCGAAT
TTATAAAGGAAGCCAGCCAGGGAAAAAGCAGCTCTGCTCAGCGCAGCACTGTCTGCGGGGAAGGTCACCATTGACAGCAGCTATGACATTT
GCCAAGATATCCCAACACCTGGATTTTCATTAGCATCATGACCTACGATTTTCATGGAGCCTGGCGTGGGACCACAGGCCATCACAGTCCCCTGT
TCCGAGGTCAGGAGGATGCAAGTCCTGACAGATTACGCAACACTGACTATGCTGTGGGTACATGTTGAGGCTGGGGCTCCTGCCAGTAAGC
TGGTGTGGGCATCCCCACCTTCGGGAGGAGCTTCACTCTGGCTTCTTCTGAGACTGGTGTGGAGCCCCAATCTCAGGACCGGGAATTCCAGG
CCGGTTCACCAAGGAGGCAGGGACCCCTTGCTACTATGAGATCTGTGACTTCTCCGCGGAGCCACAGTCCATAGAATCCTCGGCCAGCAGGT
CCCCATGCCACCAAGGGCAACCAGTGGGTAGGATACGACGACCAGGAAAGCGTCAAAGCAAGGTGCAGTACCTGAAGGACAGGCAGCTG

```

GCGGGCCCATGGTATGGGCCCTGGACCTGGATGACTTCCAGGGCTCTTCTGCGGCCAGGATCTGCGCTTCCCTCTCACCAATGCCATCAAGG
ATGCACTCGCTGCAACGTAGCCCTCTGTTCTGCACACAGCACGGGGGCAAGGATGCCCCGTCCCCTCTGGCTCCAGCTGGCCGGGAGCCTG
ATCACCTGCCTGTGTAGTCCAGGCTGAGCCTCAGTCTCCCTCCCTTGGGGCCTATGCAGAGGTCCACAACACACAGATTTGAGCTCAGCCCT
GGTGGGCAGAGAGGTAGGGATGGGGCTGTGGGGATAGTGAGGCATCGCAATGTAAGACTCGGGATTAGTACACACTTGTGATTAATGGAAA
TGTTTACAGATCCCCAAGCCTGGCAAGGGAATTTCTTCAACTCCCTGCCCCCAGCCCTCTTATCAAAGGACACCATTITGGCAAGCTCTATC
ACCAAGGAGCCAAACATCTTACAAGACACAGTGACCATACTAATTATACCCCTGCAAAGCCAGCTTGAAACCTTCACTTAGGAACGTAATC
GTGTCCCTATCCTACTTCCCTTCTAATTCCACAGCTGCTCAATAAAGTACAAGAGCTTAACAGTGAAAAAAAAAAAAAAAAAAAAAAAAAAAA
AAAAA

```

2.6 TaqMan gene expression array

To reveal a potential pathway of CHI3L1 in regulating VSMCs, a set of differential gene expression analyses using Custom TaqMan Gene Expression Array Plates (Applied Biosystems, Pleasanton, CA) were performed. First, we utilized the powerful bioinformatic tool RegRNA2.0 as described above to predict those potential effectors based on dynamic programming and computing free energy. Here, 19 candidates were obtained through this bioinformatics analysis with predicted binding free energy of less than -20 Kcal/mol. (see Fig 10).

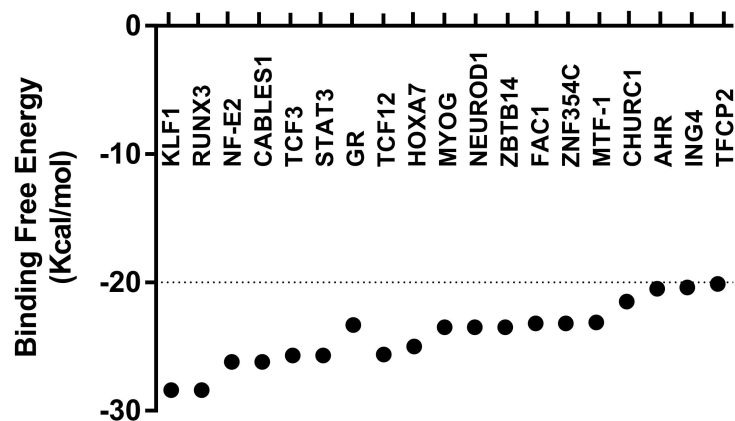


Fig 10. Predicted Panel of Effectors potentially interacting with CHI3L1. All selected candidates exploiting a binding free energy below -20 Kcal/mol.

Further, these 19 downstream candidates – together with four genes associated with VSMC phenotypic switching, five genes associated with VSMC apoptosis, and four endogenous control genes – were designed and assessed through real-time PCR using Custom TaqMan Gene Expression Array Plates (Applied Biosystems, Pleasanton, CA) containing gene-specific primers (see Table 7). The total RNA was collected from triplicate wells of VSMC using the RNeasy Plus Mini Kit (Qiagen, Hilden, Germany). Then, reverse transcription was synthesized using a High Capacity RNA-to-cDNA Kit (Thermo Fisher, Vilnius, Lithuania). Furthermore, according to the manufacturer’s instructions, we combined the cDNA and TaqMan Fast Advanced Master Mix (Life Technologies, Austin, TX). Next, each well of our TaqMan Array Plates was

reconstituted using 20µl of cDNA-Master Mix and then performed under the StepOnePlus Real-Time PCR System (Life Technologies, Singapore) with the following cycling conditions: 50°C and 2 mins for UNG (Uracil-N-Glycosylase) incubation, 95°C and 10 mins for enzyme activation, 95°C and 15 sec for denature, followed by 40 cycles of 60°C and 1 min for the final extend. Results were analyzed using the relative quantification $\Delta\Delta$ Ct method. Further statistical analysis was performed with GraphPad Prism 7 (GraphPad Software Inc, San Diego, USA).

Gene	ID	Gene	ID
KLF1	Hs00610592_m1	NR3C1/GR	Hs00353740_m1
RUNX3	Hs01091094_m1	KLF4 1	Hs00358836_m1
NF-E2	Hs00232351_m1	RUNX2	Hs01047973_m1
CABLES1	Hs01106667_m1	OCT_4	Hs04260367_gH
TCF3	Hs01012685_m1	MYOCD	Hs00538076_m1
STAT3	Hs00374280_m1	CDKN1A 2	Hs00355782_m1
TCF12	Hs00918966_m1	c-myc	Hs00153408_m1
HOXA7	Hs00600844_m1	Bcl2	Hs00608023_m1
MyoG	Hs01072232_m1	Bax	Hs00180269_m1
NEUROD1	Hs01922995_s1	TP53	Hs01034249_m1
ZBTB14	Hs01924092_s1	18s 3	Hs03003631_g1
ZNF354C	Hs00395825_m1	GAPDH	Hs02786624_g1
MTF-1	Hs00232306_m1	HPRT	Mm03024075_m1
CHURC1	Hs00540886_m1	GUSB	Hs00939627_m1

Table 7. Assay Identifications for Genes used in custom TaqMan Gene Expression

Arrays. 1. Genes associated with VSMC phenotypic switching; 2. Genes associated with VSMC apoptosis; 3. Endogenous control genes (housekeeping). KLF1(Krüppel-like factor-1), RUNX3(RUNX Family Transcription Factor 3), NF-E2(nuclear factor erythroid-2), CABLES1(Cdk5 and Abl enzyme substrate 1), TCF3(Transcription Factor 3), STAT3(Signal transducer and activator of transcription 3), TCF12(Transcription Factor 12), HOXA7(Homeobox A7), MyoG(Myogenin), NEUROD1(Neuronal Differentiation 1), ZBTB14(Zinc Finger And BTB Domain Containing 14), ZNF354C(Zinc finger 354C), MTF-1(metal regulatory transcription factor 1), CHURC1(Churchill Domain Containing 1), NR3C1/GR(glucocorticoid receptor gene), KLF4(Kruppel Like Factor 4), RUNX2(Runt-related transcription factor 2), OCT_4(octamer-binding transcription factor 4), MYOCD(Myocardin), CDKN1A(Cyclin Dependent Kinase Inhibitor 1A), Bcl2(B-cell lymphoma 2), Bax(BCL2 Associated X), TP53(cellular tumor antigen p53), GAPDH(Glyceraldehyde 3-phosphate dehydrogenase), HPRT(Hypoxanthine-guanine phosphoribosyltransferase), GUSB(Glucuronidase Beta)

2.7 Transcription factor prediction

To date, bioinformatic algorithms were developed to predict the target's transcription factor based on the protein-mRNA or miRNA-mRNA interaction rules. Here, the Gene Cloud of Biotechnology Information (GCBI) (Shanghai, China, <https://www.gcbi.com.cn>) (Yu 2012) is one of these powerful algorithms. The GCBI online laboratory is a powerful platform that provides data services, molecular information solutions, and cloud genetic analysis. It is a widely used platform containing differentially expressed gene (DEG) analysis, GO (gene ontology) enrichment analysis, pathway network analysis, and gene signal network analysis (Huang 2018). In this thesis, the promoter sequences were retrieved from the Ensembl database (<http://www.ensembl.org>), and the target promoter sequences were obtained 1000 base pairs upstream from the transcription start site (TSS) of the CHI3L1 transcript (see Table 8). Next, the GCBI program retrieves all human protein coding genes and computes them.

The method GCBI uses is based on the TRANSFAC database (Matys 2006), COSMIC database (Forbes 2011), and the Single Nucleotide Polymorphism Database (dbSNP) (Wheeler 2007). Here, the TRANSFAC database is organized by position weight matrices (PWMs) that it is centered around the interaction between transcription factors (TFs) and their DNA binding sites (TFBS) (Morozov 2013). Additionally, related TFs are screened by computing an algorithm named position-specific scoring matrix (PSSM): the closer to 1 the score value is, the more likely it is a target. Further, the COSMIC database and dbSNP assist in identifying either DNA methylation marks or single nucleotide polymorphisms (SNPs) in their TF-DNA binding area of the CHI3L1 translated region. Taken together, possible TFs were eventually analyzed and reported through the in-built evaluation model provided by GCBI (Fig11).

Table 8. Sequence of the proximal promoter of CHI3L1

>chromosome:GRCh38:1:203178331:203187749:-1
TCACCTACTGCCTATTAATTAATGTTAAGCCTGCAAAGAATGGAGTTGTCCTGGATATTTGGCCAAAAAAAAAATGTATCCACAAACAGGGAC
GTAATCAGGCAGGGAGCCTCGTTAAGAAGTTTGTTCCTTGTCCTAGGAGTGATGAGAGATCACTGAAGGATTTAGAGAGGGGCTGTATCATCA
GGCTTGGGTTCCAAAGCCTCACTGAGAGAGTTGGGGAGCTGACTGATGTGATGCTCGTGAGCCGCCCGTAGGGCTGTATTTCCTCCAT
GGTGCCTCACTGCAGCACCGAGCTTGCAAAAAGATCCTCTCTCTTTATGGGAATTTCAAAACAGAAGCAAAATAGCACCGGGGCTTAAAGCATI
CTTGGGAATTTCCCTGTCTTTCCCTCTAAATAATCAGCATGTAATTTGCAAAAAAAAAAAAAAAAAAAAAAAAAAAGACACGGGCCAAAAAG
GGAGCGCTCAGTTTCAGGCTCTTTGCTTTCTTCTCCCGAGGCTCTCTGGCCCTTACCCAGCCTGAAGACAGAAAGTGTGAGGGGGAGGGTAG
GAAGGTAGGTCAAGCAGGGCAATGCTGAGCCTGGGAAGAAAACAACAGCCTTGTTTAGGGCACTGTGGCTTACGTAACATAAATGTGCCCCAG
TTTCCACCTGGCCAGGGGCTGGAGTGAATGCTGAAAGATGCAAAGGTAGAGGCTGCCAGAAAAAGCCAGGAAATGTGTTGGCAAGAAAAGGCCAG
TGGTGGGGTGCAGGAGTGGGAGGAAGGCTGGGAAATGCGGCTGAGTCACATCTCCAGAAGCCCCCATCATCACCTTAGTGGCTCTTCTGTCTG
GCAGGTGCCTCATGAAGACCTGACCCAAAGTTTCAAAACTGCGGTTTCTCAACCTCTCTGGTAATCCATAGTACTCCCCCGCTCCACTI
TGCCAGCCTCGTGATTCCTTTCATTGACACATAGCTCAGTTCCCATAAAAGGGCTGGTTTGCCCGCTCGGGG

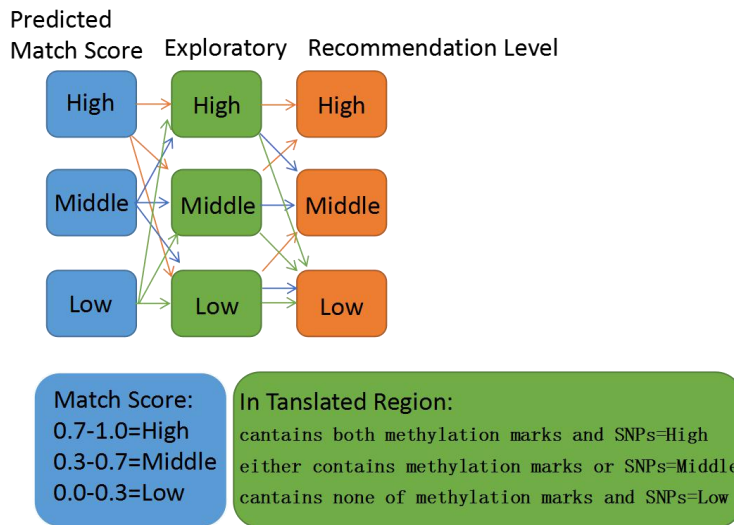


Fig 11. Schematic predictive evaluation model from GCBI online program. A predicted TF with a good score value and DNA methylations or SNPs in its binding area is considered a high recommendation level.

2.8 Statistical analysis

Statistical analysis was carried out using GraphPad Prism 7 (GraphPad Software Inc, San Diego, USA). Normal distributed samples were analyzed using an independent t-test for $n=2$ and ANOVA test for $n>2$. Non-parametric data were used in the Mann-Whitney-U-test for $n=2$ and Kruskal-Wallis for $n>2$. Continuous data in qRT-PCR results are presented as mean \pm SD. Differences of RNA level expression were calculated as fold change versus control using the mean Δ Ct defined as Ct value of target RNA minus Ct value of endogenous control. The significance of differences * for $p<0.05$; ** for $p<0.01$; *** for $p<0.001$ were considered statistically significant.

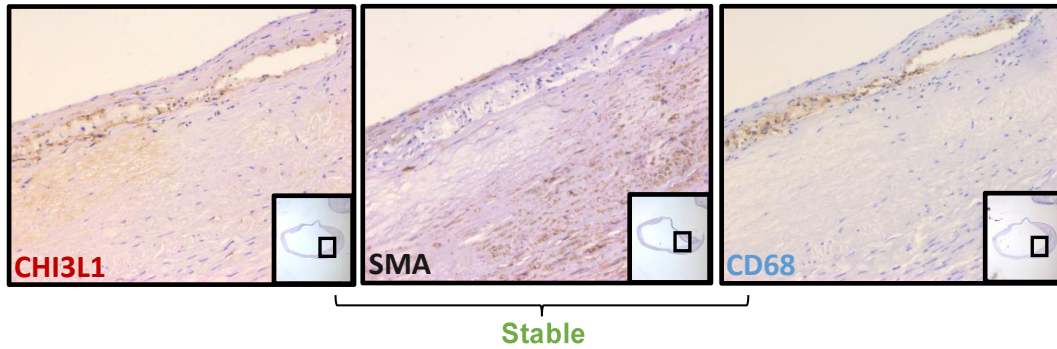
3. RESULTS

3.1 Immunohistochemical analysis of CHI3L1

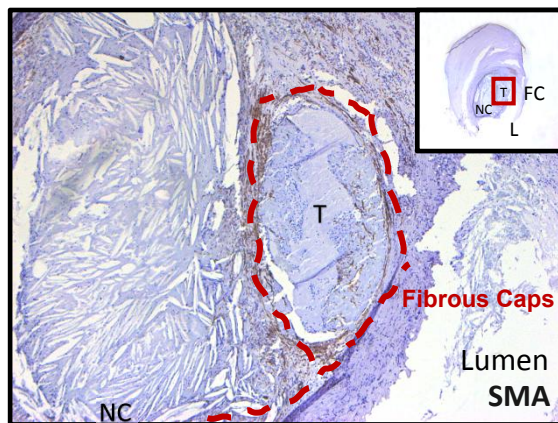
Previous transcriptome array results have shown that CHI3L1 was the most significantly upregulated transcript in rupture plaques. Next, in our ex vivo study, anti-CHI3L1 immuno-expression was performed to confirm the affiliation of CHI3L1 with cells in human carotid plaques. Here, α -SMA positive and CD68 positive cells were presumed to be of VSMCs and macrophage ($M\Phi$), respectively. In stable plaques, CHI3L1 were expressed in both VSMCs and $M\Phi$ s (Fig.12 A). Additionally, a representative rupture sample involving a clear fibrous cap over a lipid core was selected for further consecutive staining of cellular localization and CHI3L1 expression as well (Fig.12 B). In these rupture plaques, α -SMA and CD68 positive cells were both positive for CHI3L1, and also major in putative macrophages.

Furthermore, when observed closely, anti-CHI3L1 immuno-expression were increased in rupture plaque when compared to stable plaques, and those increased CHI3L1/ α -SMA positive cells seemed to be mainly located in the fibrous cap and the non-uniform thickening area of media/neointima (Fig.12 C). Later, plaques were further stained with antibodies against ki67 and caspase-3. And CHI3L1/ α -SMA positive cells appeared to be hyperproliferative (Ki67+) in unstable plaques (Fig.12 D).

A

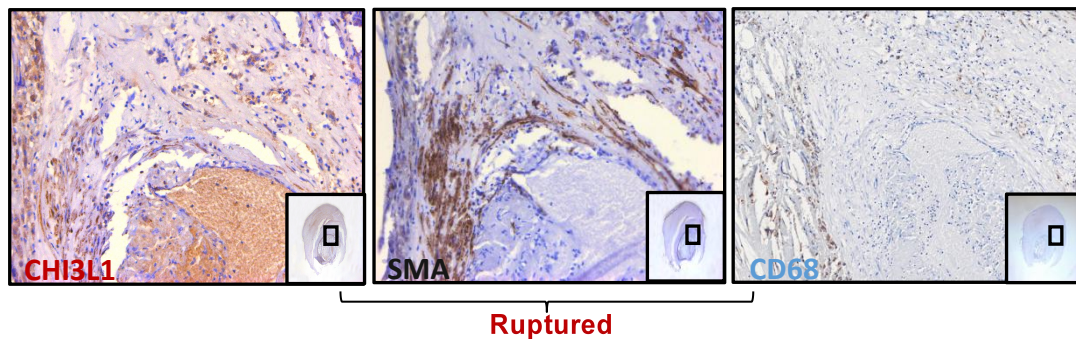


B



10x

C



D

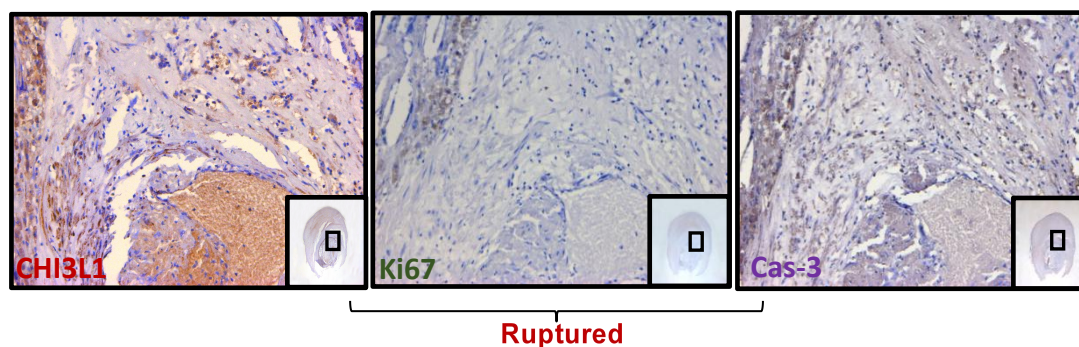


Fig 12. Immunohistochemical staining of CHI3L1 on sections of carotid plaques.

(A) In stable plaques, CHI3L1 was mainly expressed in CD68+ cells. (B) An overview of the representative rupture plaque by performing α -SMA staining. FC=fibrous cap; T=thrombus; NC=necrotic core; L=lumen. 10x resolution. (C) In rupture plaques, CHI3L1/ α -SMA+ cells seemed to mainly express in the fibrous cap and the neointima thickening area. (D) CHI3L1/ α -SMA+ cells appeared hyperproliferative (Ki67+) in rupture plaques. 20x resolution.

3.2 Analysis of CHI3L1 modulation at mRNA level in VSMC

For quantification of CHI3L1 modulation at the mRNA level in primary patient-derived VSMCs, qRT-PCR analysis was performed. First, to obtain reproducible and reliable results, a transfection optimization with reasonable efficiency was established; then, we explored the modulation of CHI3L1 in VSMC phenotypic switching. These results are described in greater detail in the following sections.

3.2.1 Efficiency of CHI3L1 modulation in VSMCs

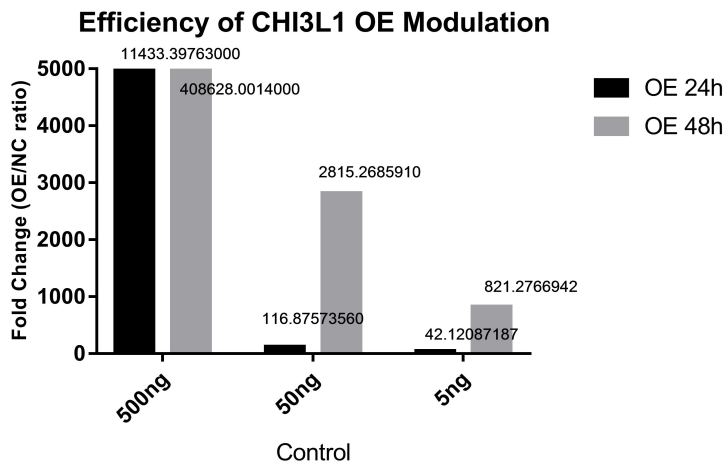
Due to a greater proliferation and identity, Passages 4–6 were selected for all further experiments. Thereafter, transfected cells with the target modulation in 6-well plates were collected and thermo-cycled for amplification to detect CHI3L1 expression. The normalized threshold cycle (Ct) value of each gene was obtained from a housekeeping gene, RPLP. The relative amount of each mRNA was also normalized to RPLP.

In the case of CHI3L1 overexpression modulation, different amounts of recombinant plasmid were examined over time. Here, 5ng/ μ l seemed to be the optimal concentration with a 42 folds upregulated at the 24-hour point and over 600 folds upregulated at the 48- time point ($P=0.0148$, $n=3$) (Fig.13 A). We assumed that it was more reasonable to reflect the characterizing gene involvement in a disease situation. Validated results based on technical and biological replicates were significant, as shown in Figure.13 C.

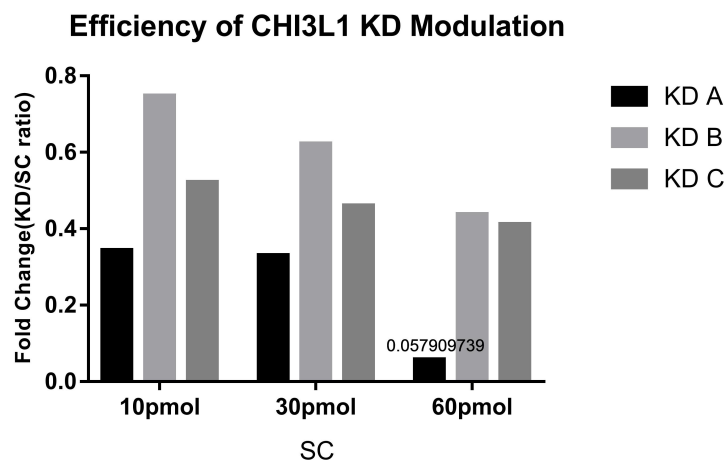
Furthermore, in an efficient study of CHI3L1 knockdown modulation, by targeting against CHI3L1 gene in VSMCs, all three synthesized siRNA oligos can sufficiently

suppress CHI3L1 expression at different concentrations when compared to the scrambled control. However, we identified that a concentration of 60pmol (20nM) of variant A has the best efficiency out of three by silencing the expression of CHI3L1 over 85% 48 hours after we transfected into VSMCs ($P=0.0007$, $n=3$) (Fig.13 B). The validation based on technical and biological replicates was also significant (Figure 13 C).

A



B



C

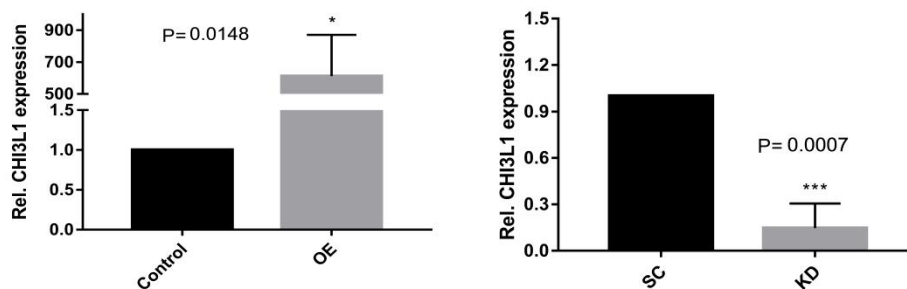


Fig 13. qRT-PCR validation of CHI3L1 modulation in VSMCs (A) The representative bar chart of the overexpression modulation of CHI3L1 and the mRNA expression level of CHI3L1

was over 42 folds higher at the 24-hour time point and over 800 folds higher than control group – an amount of 5ng – at the 48-hour time point, respectively. (B) The representative bar chart of the knockdown modulation of CHI3L1, where gene silencing analysis showed that variant A was the most effective vector at a concentration of 60pmol. (C) Validation of CHI3L1 modulation in VSMCs, the overexpression group vs the control group (P=0.0148,n=3); the knockdown group vs the scramble group (P=0.0007, n=3). Data were presented as the mean±SD; *P<0.05; **P<0.01; ***P<0.001.

3.2.2 Exploring role of CHI3L1 in VSMC phenotypic switching

Vascular smooth muscle cell phenotype switching has been considered to play a vital role in vascular disease development. To explore whether CHI3L1 may influence VSMC phenotype switching, two typical phenotypic biomarker expression levels were determined by qRT-PCR in primary patient-derived VSMCs treated with CHI3L1 modulation for 24 hours. Results disclosed that silencing CHI3L1 can significantly suppress the mRNA expression of VSMC markers ACTA2 (α -SMA), while simultaneously increasing the mRNA expression of macrophage markers CD68 (Fig.14 A). However, in contrast, overexpressing CHI3L1 did not significantly alter these endogenous gene expressions (Fig.14 B). The results of trans-differentiation may provide evidence of the role CHI3L1 plays in VSMC phenotypic switching.

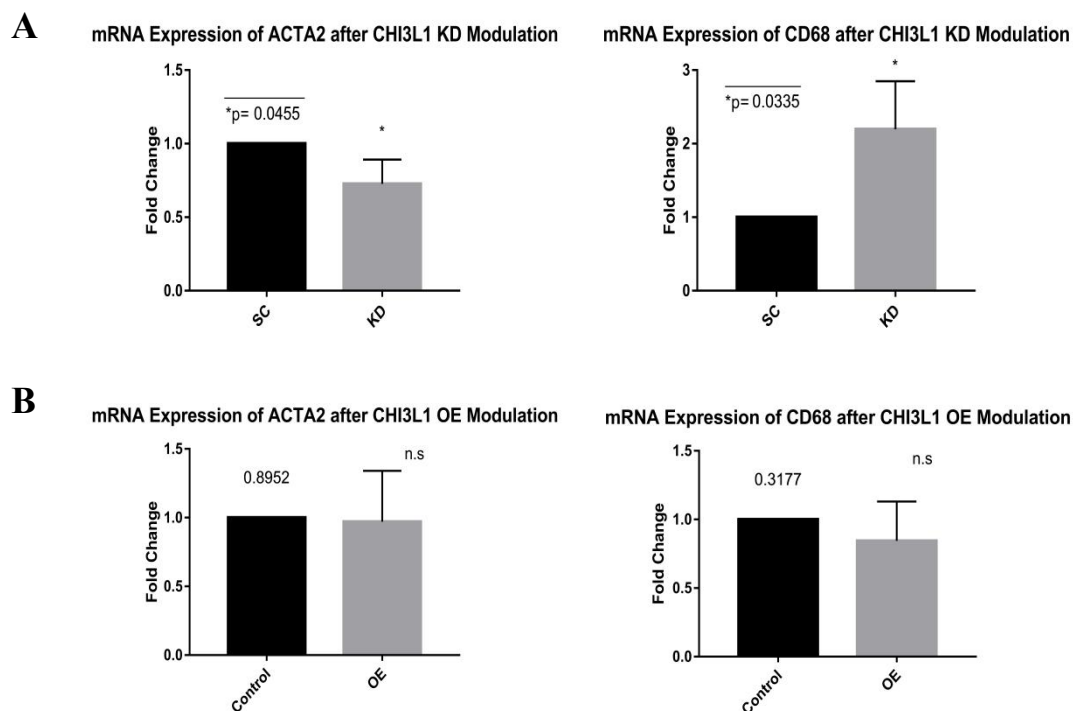
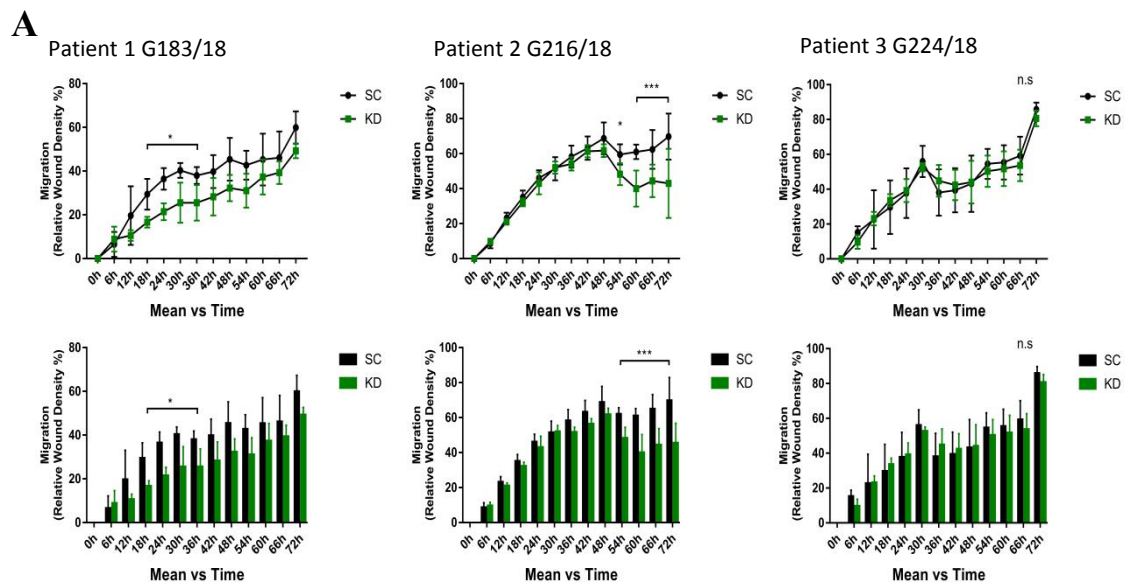


Fig 14. Phenotypic biomarker expression after CHI3L1 modulation: (A) Relative mRNA levels of the VSMC biomarker ACTA2 (α -SMA) were significantly reduced in VSMCs transfected with the CHI3L1 inhibitor (P=0.0455, n=3). Meanwhile, the macrophage biomarker (CD68) was displayed significantly upregulated (P=0.0335, n=3). (B) Conversely, analysis showed no significant difference in relative phenotypic biomarker expression after CHI3L1

overexpression (P=n.s, n=3). Expression of relative mRNA was measured by qRT-PCR, normalized to RPLP, and expressed as fold change. Data and error bars represent the mean±SD. *P<0.05 (versus control/scramble); n.s, non-significant. Each experiment is representative of three independent studies.

3.3 CHI3L1 knockdown inhibits migration in VSMCs

Once the transfection setup was ready, we then implemented all further experiments. By using the IncuCyte Scratch Wound Assay module, differences in cell morphology and rate of wound closure between migrating VSMCs after CHI3L1 modulation were observed. As shown in Fig.15 A, cell migration were measured using relative wound density in percentage between initial wound and incremental wound closure for 72h. Since cells derived from different patients can behave differently in culture conditions depending on the genetics and age of the individuals, we therefore demonstrated the results from three individual samples respectively, which indicated that silencing CHI3L1 can decrease the migration in two out of three experiments. Furthermore, we analyzed cell movement after CHI3L1 overexpression modulation and found that there was no significant difference between the overexpression and control groups (Fig.15 B). There is further evidence suggesting a role of knockdown CHI3L1 may reduce VSMC migration.



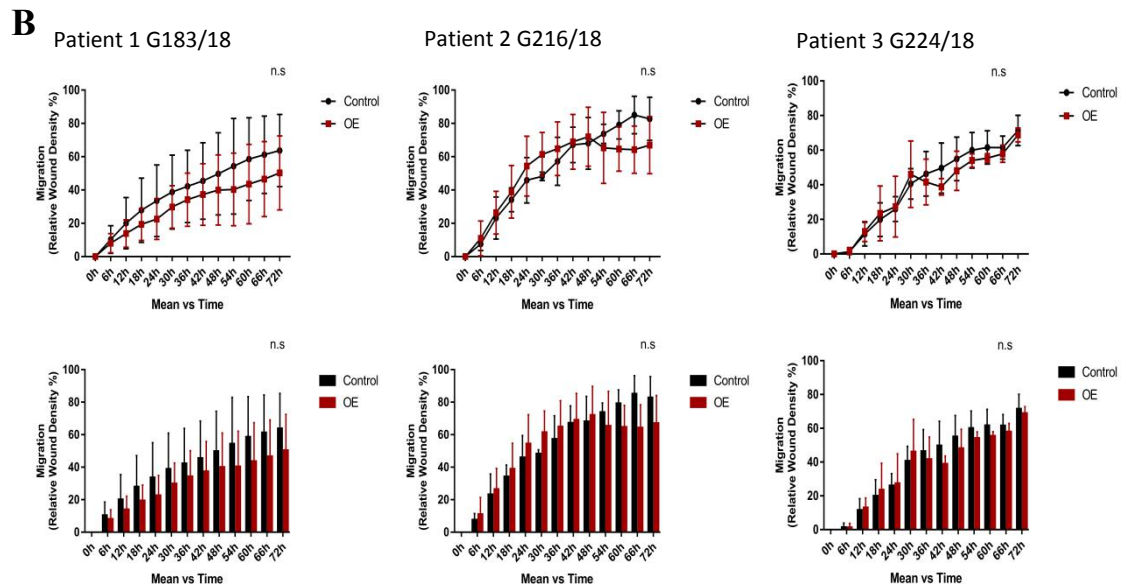
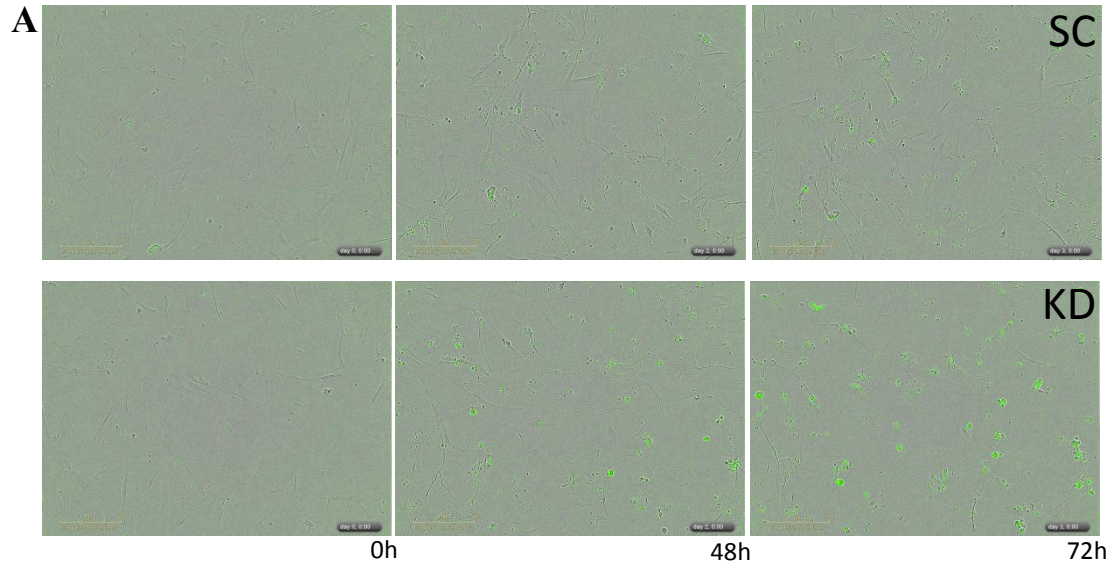


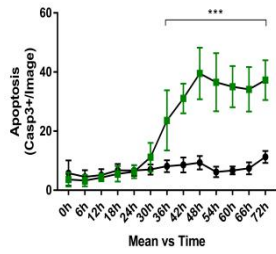
Fig 15. Migration in VSMCs after CHI3L1 modulation: (A) Quantification of cell migration by measuring relative wound density in percentage – silencing CHI3L1 can significantly decreased migration in VSMC in two out of three independent experiments at certain timepoints, n=3. (B) There was no significant difference between the overexpression and normal control groups n=3. Data were presented as the mean±SD. *P<0.05; **P<0.01; ***P<0.001, n.s, non-significant.

3.4 CHI3L1 knockdown induces apoptosis in VSMCs

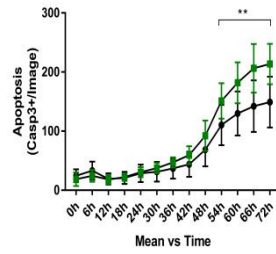
By reading the green fluorescent label of the IncuCyte Caspase 3 Reagent – which is a reliable marker for apoptosis and also compatible with the IncuCyte live-cell analysis system – we then quantified the apoptosis after CHI3L1 modulation in primary patient-derived VSMCs as described above (G183/18, G216/18, G224/18). In measurements over a total of 72 hours, Fig.16 A showed that knockdown CHI3L1 can significantly induces VSMC apoptosis in all three independent experiments. However, in the case of CHI3L1 overexpression, there was no difference of green-fluorescence signaling between the overexpression and control groups in the apoptosis of VSMCs (Fig.16 B).



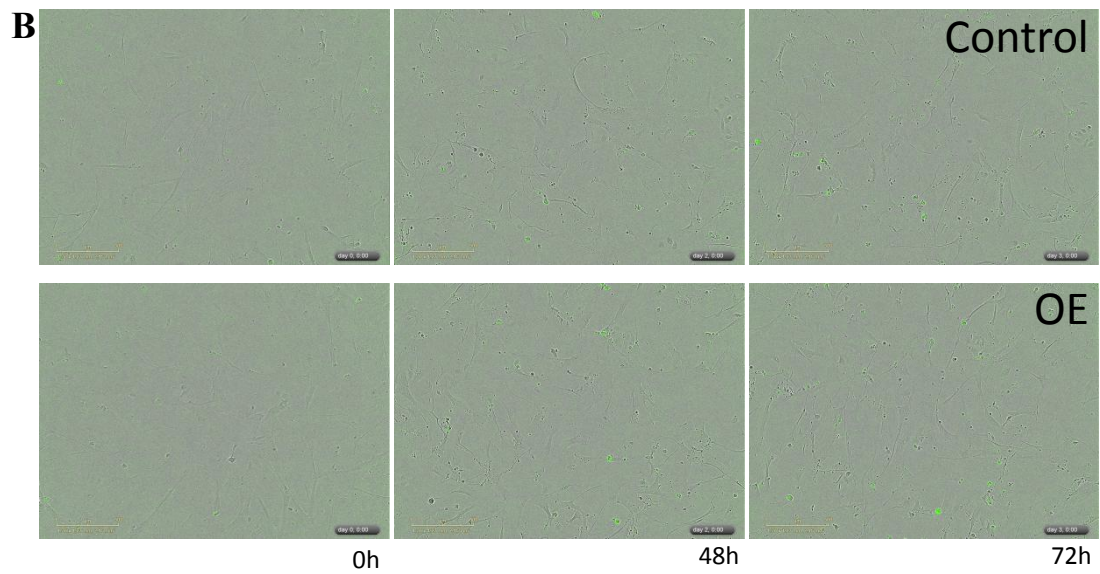
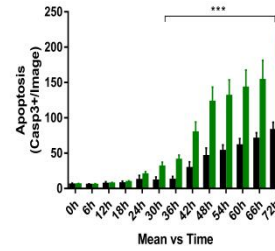
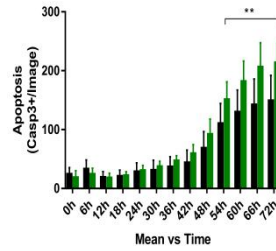
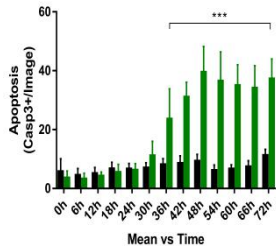
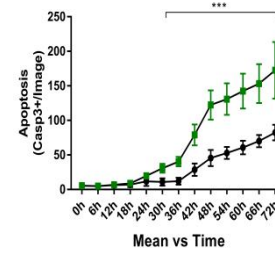
Patient1 G183/18



Patient2 G216/18



Patient3 G224/18



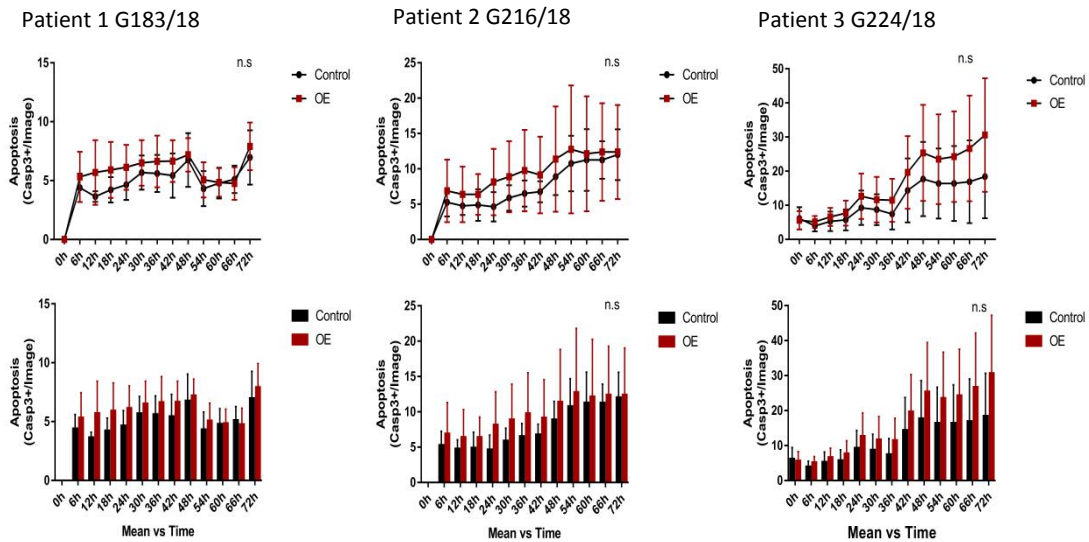
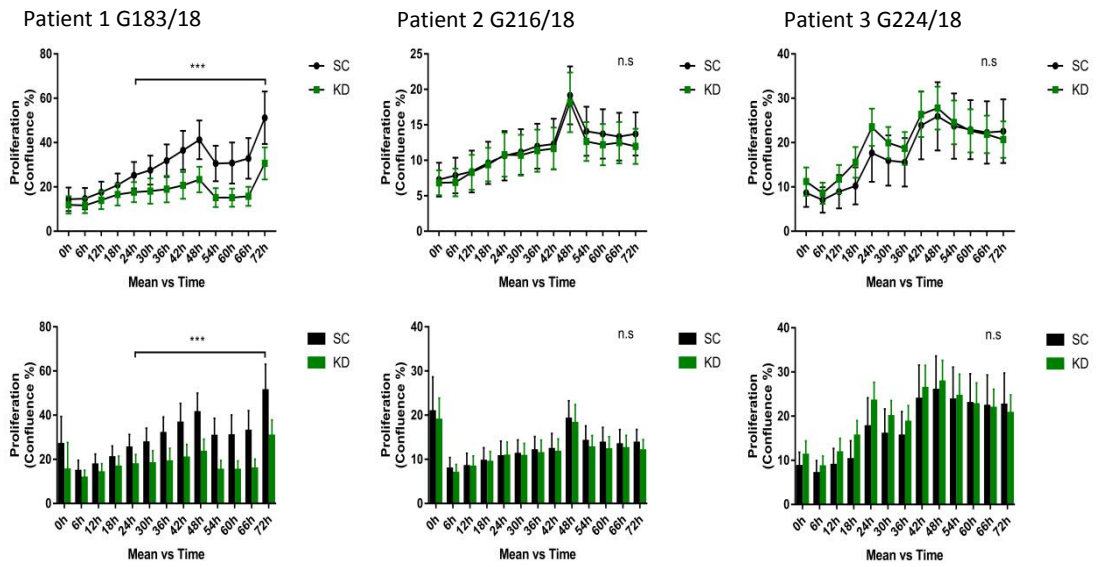
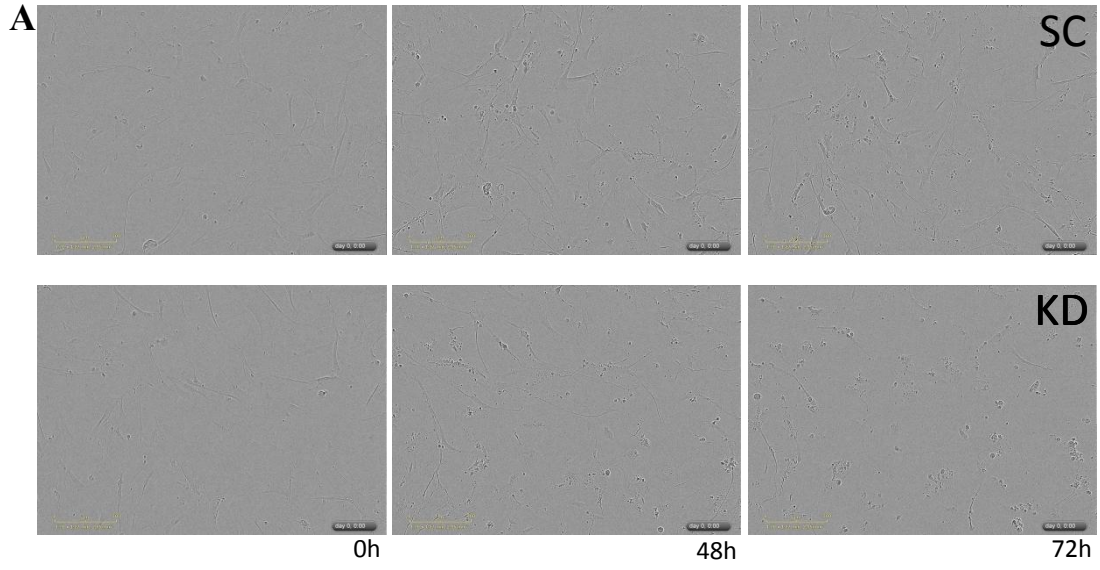


Fig 16. Apoptosis in VSMC after CHI3L1 modulation: (A) Upper panels: Representative phase-contrast and green-fluorescence merged images taken 0, 48, and 72 hours after CHI3L1 modulation. Compared to the scramble groups, CHI3L1 knockdown groups demonstrated greater fluorescent cells. Lower graph: Green cell counts up to 72 hours after CHI3L1 modulation. These graphs represent one of the replicates. Each point represents the mean of the caspase-3 counts for four different optic fields analyzed per well and treatment at a given time point. In all three replicates, silencing CHI3L1 can significantly induced the apoptosis in VSMCs, $n=3$. (B) However, there was no significant difference in apoptosis between the overexpression and control groups, $n=3$. Data were presented as the mean \pm SD; * $P<0.05$, ** $P<0.01$, *** $P<0.001$, n.s, non-significant.

3.5 CHI3L1 knockdown reduces proliferation in VSMCs

Alongside apoptosis within the same well, VSMC proliferation under CHI3L1 modulation was captured with the IncuCyte Cell Proliferation Assay module. By analyzing the occupied area (%confluence) of each cell image over time, cell proliferation was monitored and quantified. Of these results, the normalized ones showed a significant reduction of proliferation in VSMCs after CHI3L1 knockdown modulation in one out of three replicates(Fig.17 A). Meanwhile, we found that overexpressing CHI3L1 does not affect the proliferation of VSMCs *in vitro* (Fig.17 B).



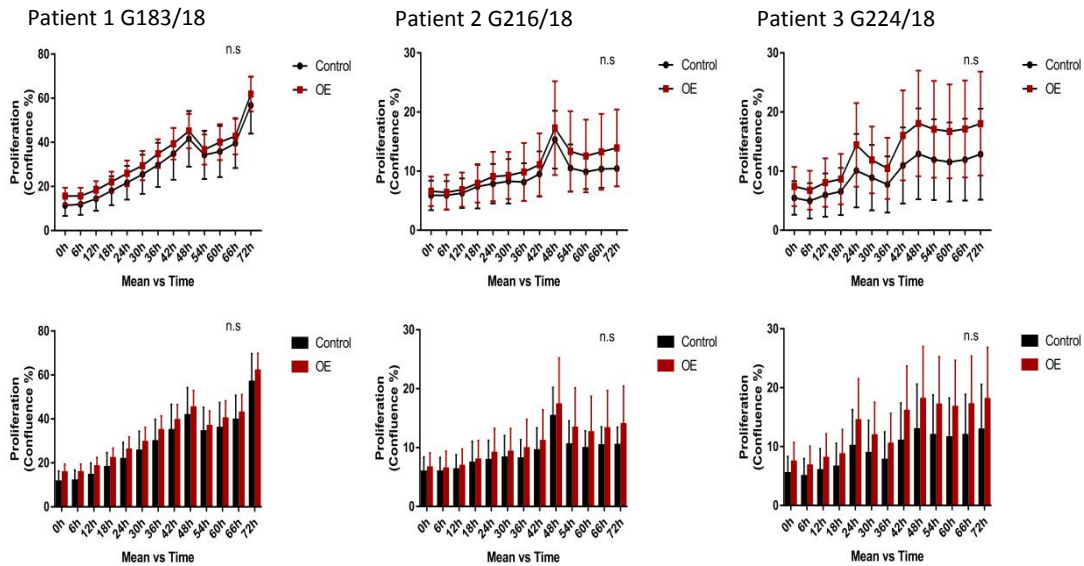
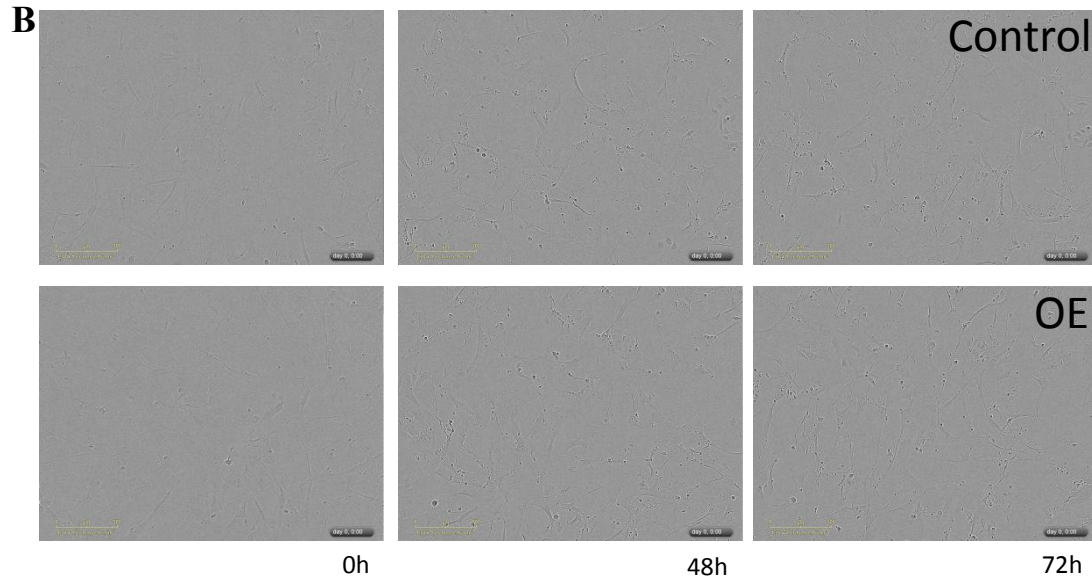


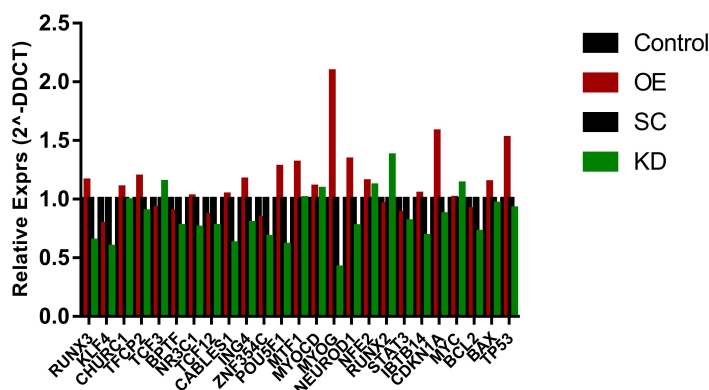
Fig 17. Proliferation in VSMC after CHI3L1 modulation: (A) Upper panels: Representative phase-contrast images taken at 0, 48, and 72 hours after CHI3L1 modulation. Compared to scramble groups, CHI3L1 knockdown groups show a greater occupied area of VSMCs. Lower graph: Cell confluence analysis up to 72 hours after CHI3L1 modulation. These graphs are representative of one of the replicates. Each point represents the mean of the confluence percentages for four optic fields analyzed per well and treatment at a given time point. Based on three biological replicates in primary patient-derived VSMCs, silencing CHI3L1 can significantly reduce the proliferation in VSMCs in one out of three replicates, $n=3$. (B) By measuring the object confluence of each cell images, there was no significant difference between the overexpression and control groups, $n=3$. Data were presented the mean \pm SD. * $P<0.05$; ** $P<0.01$; *** $P<0.001$, n.s, non-significant.

3.6 Potential mediators of CHI3L1 modulation

Identifying CHI3L1-mediated genes may determine VSMCs' survival and phenotypic modulation, so we performed custom TaqMan gene expression array analysis to measure gene expression changes in CHI3L1 modulation VSMCs. Here, we show the average of relative mRNA expression of each gene from four replicate arrays in the bar charts below. Among 28 candidate genes, only MyoG (Myogenin), a muscle-specific transcription factor that can induce myogenesis in a variety of cell types in tissue culture (Moresi 2010), was significantly correlated with CHI3L1 overexpression or inhibition (see Fig. 18 B C). Furthermore, KLF4, a key regulator in VSMCs phenotypic switching (Shankman 2015), was significantly down-regulated in CHI3L1 knockdown modulation (see Fig. 18 C). Although positive results here are rather limited, an analysis still showed a number of genes altered by CHI3L1 with relative corresponding changes, suggesting their potential roles in CHI3L1-mediated VSMC cell survival and phenotypic transition (see Fig. 18 A). For example, four genes can be induced by CHI3L1 overexpression: MyoG (2.1-fold), CDKN1A (1.6-fold), TP53 (1.5-fold), and POU5F1 (1.30-fold), when compared to the expression level of housekeeping genes (see Fig. 18 B). In contrast, their expression revealed lower levels in CHI3L1 knockdown modulation: MyoG (0.68-fold), CDKN1A (0.86-fold), TP53 (0.91-fold), and POU5F1 (0.60-fold) (see Fig. 18 C). Of these, POU5F1 (POU Class 5 Homebox 1 also known as Oct4) – together with KLF4, MYOCD, and RUNX2 – has been considered a key mediator in VSMC phenotypic switching (Leeper 2018). Additionally, CDKN1A (p21) and TP53 (p53) are well-known cell fate associated genes. Although it is barely a compelling result, it still provides evidence that CHI3L1 may regulate VSMC survival and phenotypic switching in some way, which we discuss in more detail below (see Discussion).

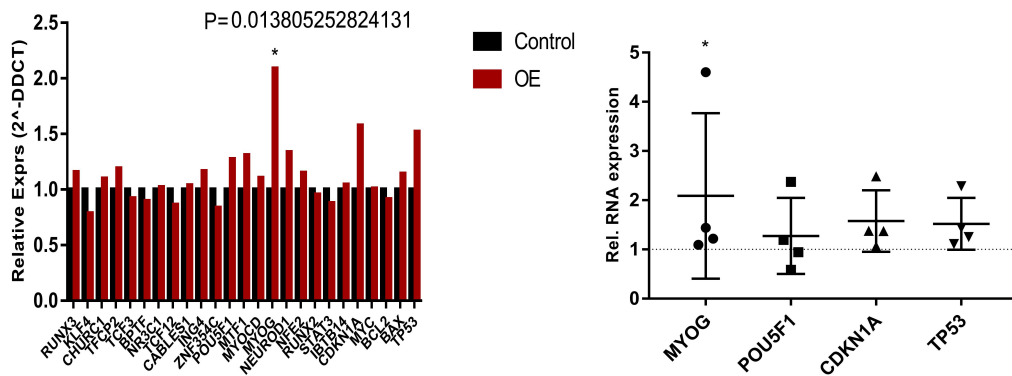
A

TaqMan Array Plates after CHI3L1 Modulation



B

TaqMan Array Plates after CHI3L1 OE Modulation



C

TaqMan Array Plates after CHI3L1 KD Modulation

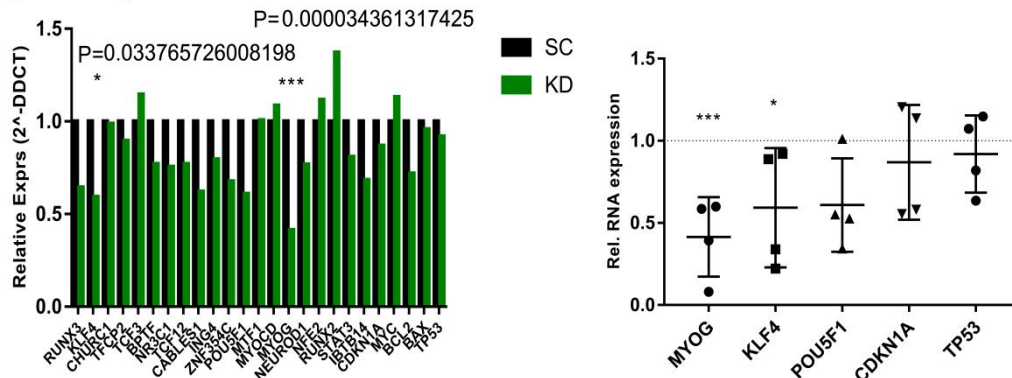


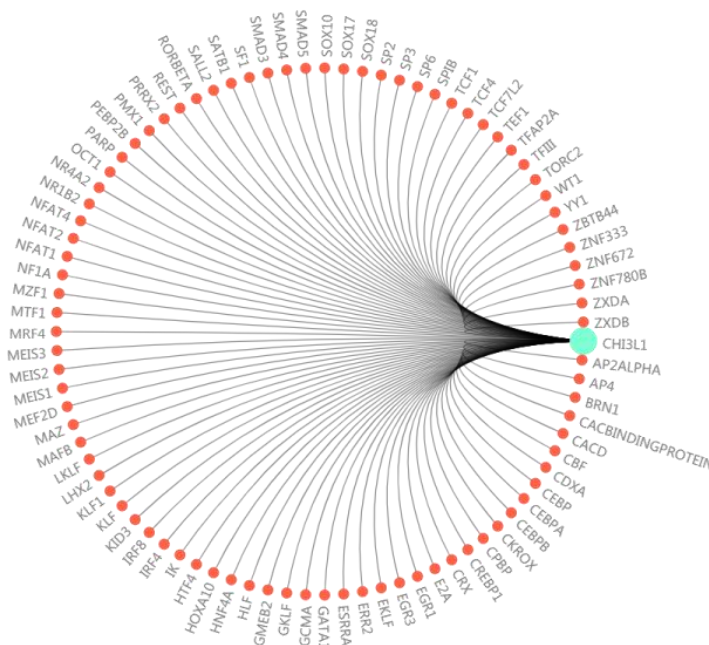
Fig 18. Relative Expression of Genes in VSMC after CHI3L1 Modulation using TaqMan Array Plates: (A) The average of relative mRNA expression of genes in CHI3L1 modulation – a number of genes, including MyoG, POU5F1, CDKN1A and TP53, showed corresponding change. (B) The average of relative mRNA expression of genes in CHI3L1 overexpression modulation with no statistical significance in four replicates analysis. (C) The average of relative mRNA expression of genes in CHI3L1 knockdown modulation – only MyoG showed a significantly reduction altered by silencing CHI3L1 (P=0.00061, n=4). *P<0.05; **P<0.01; ***P<0.001, n.s, non-significant.

3.7 Prediction of transcription factors interacting with CHI3L1

To reveal the potential transcription factor of CHI3L1, we used the GCBI program as described above. Here, a predicted transcription factor with a good score value and either DNA methylations or SNPs in its binding area was considered as a high recommendation. In Fig.19 A, among all human transcripts, eventually 86 TFs were evaluated as high level and reported by the GCBI program. Additionally, we manually selected the top 10 TFs, which exhibited better binding affinity and exploration (Fig18 B). Of these, CREBP1 was the most likeliest transcription factor to interact

with CHI3L1. Further experiments, such as the Luciferase reporter assay and chromatin immune precipitation (ChIP) should be performed to confirm the result and map a regulatory network of CHI3L1 in the future.

A



B

Name	Alignment	Match Score	Region contains methylation marks	Region contains SNPs	Numbers of Motif on target sequence
CREBP1	ttaCGTAA	1	+	+	1
GMEB2	tTACGTaa	1	+	+	1
HLF	agttaCGTAAgc	0.997	+	+	1
CPBP	acGGGGC	1	+	-	6
NFAT1	tTTTCC	1	-	+	6
SF1	CAAGGtca	1	-	+	3
NFAT4	tTTTCC	1	-	+	3
PMX1	tTATTA	1	-	+	2
REST	agcACCTT	1	-	+	1

Fig 19. The Analysis of CHI3L1 Transcription Factors. (A) In this diagram, 86 targets were enriched from the GCBI analysis, and each orange dot was evaluated as a high recommendation level based on the predictive evaluation model, and thus represents putative TFs of CHI3L1. (B) The top 10 out of 86 potential alignments that deserve further investigation.

4. DISCUSSION

The conventional view of plaque vulnerability leading to rupture in advanced atherosclerosis has been associated with a thin or disrupted fibrous cap; an ACTA2 (smooth muscle α -actin) positive-cells-rich layer covering the lipid core of an atherosclerotic plaque; a large population of CD68 or LGALS3 positive cells presumed to be M Φ s; and the presence of a large macrophage-derived foam-cells-rich necrotic core (Ross 1999) (Virmani 2000).

In fact, the contribution of VSMCs in atherosclerosis development and progression has been greatly underestimated (Shankman 2015). By considering therapies that allow the prevention of plaque rupture, we may be able to gain insight into the role of VSMCs within the fibrous cap. In the present study, we used a powerful technical method of LCM to precisely extract smooth-muscle-cell-enriched RNA samples from the entire fibrous cap section in pathological human carotid plaques, which allowed us to perform a whole transcriptome study to identify genes that regulate VSMC within the fibrous cap during atherosclerosis progression. CHI3L1 (chitinase-3-like-protein-1) was found to be the most significantly upregulated in rupture plaques when compared to stable plaques. Of such, transcriptome array analysis suggests a potential effect on VSMCs within the fibrous cap mediated by CHI3L1.

Interestingly, in our previous study, we also showed that CHI3L1 was a major target of miR-24, promoting aortic smooth muscle cell migration, regulating macrophage survival, and stimulating adhesion molecule expression in vascular endothelial cells (Maegdefessel 2014). Herein, as a highly conserved member of the CLPs family, CHI3L1 is expressed by a board range of cells such as SMCs, M Φ , astrocytes, endotheliocytes, and many proliferating cancer cells. Further, it has been found to be involved in many pathophysiological processes, including inflammation, tissue remodeling, tumor angiogenesis, and fibrosis (Tang 2012). Additionally, elevated serum levels of CHI3L1 serve as a biomarker in a variety of chronic inflammatory diseases (Jung 2018), and also as an independent prognostic biomarker of different cancers (Kim 2018). Furthermore, Michelsen *et al* extended these findings by demonstrating that CHI3L1 serum levels were significantly increased in patients with symptomatic carotid plaques, suggesting CHI3L1 as a promising marker of plaque vulnerability (Michelsen 2010). Similarly, Park *et al* provided evidence that serum CHI3L1 is an early surrogate biomarker for AIS patients, and its elevated expression is more significantly related to the large artery atherosclerosis (LAA) type AIS than the small vessel disease (SVO) type. Furthermore, in studies of tumor vascularization in the cancer field, CHI3L1 together with alpha-smooth muscle action (α -SMA) and vimentin expressed by SMCs or mesenchyme-derived mural cells within the out layer of the neovessels were determined to serve as a major mesenchymal cell marker in tumor angiogenesis (Phillips 2006) (Ricci-Vitiani 2008).

Consistent with previous human carotid atherosclerotic plaques studies (Michelsen 2010) (Boot 1999), our *ex vivo* (human tissue) results demonstrated that anti-CHI3L1 immuno-expression can be observed in both VSMCs (α -SMA⁺) and M Φ s (CD68⁺), prominently in M Φ s within the advanced lesions, supporting its prevalent synthesis and complex interaction between VSMC/M Φ (see Fig 12). Here, α -SMA positive and CD68 positive cells were presumed to be of VSMC and M Φ , respectively. Further, we found that CHI3L1/ α -SMA immune-expression was increased in ruptured plaques compared to stable plaques, and more importantly, these increased CHI3L1/ α -SMA positive cells seemed to be mainly located in the fibrous cap and the non-uniform thickening area of media/neointima (see Fig 12), suggesting CHI3L1 plays a role in VSMC-mediated lesion pathogenesis. Deviating from the above studies, Rocchiccioli *et al* showed a site-specific relationship between VSMC-secreted CHI3L1 and coronary atherosclerotic lesion severity by observing CHI3L1 expressed mainly in α -SMA/S100A4 positive cells (migratory VSMC with synthetic phenotype) instead of observing maximal CHI3L1 expression in M Φ s and lipid-laden M Φ s. However, our and previous studies seem to oversimplify, as ambiguity over the so-called “SMCs/M Φ s mis-identification” emerged long before and was debated extensively over the last decade (Allahverdian 2014). Given evidence that SMCs can present with M Φ markers and vice versa, it is barely possible to distinguish cells within advanced atherosclerotic lesions as solely SMC- or M Φ -derived (Feil 2014). Remarkably, over 80% of VSMCs were traditional SMC-marker negative; approximately 30% cells that would be identified as M Φ s originated from VSMCs, not hematopoietic origin; and about 18% of CD68 positive cells demonstrated a positive SMC-specific marker as well (Shankman 2015). Still, the results above provide evidence that CHI3L1 plays a role in VSMC-regulated atherosclerotic plaque vulnerability.

Given extensive clinical and laboratory observations, we investigated whether the VSMC survival effect *in vitro* (cell culture) were regulated by CHI3L1 by implementing overexpression and knockdown modulation. To address this conjecture specifically and get the closest to pathological conditions involved in lesion development for the first time, we obtained primary patient-derived VSMC from carotid atherosclerotic plaques with similar clinical characteristics and pathological features instead of culturing SMC cell lines and human primary carotid SMC derived from healthy adults. Notably, our results demonstrated silencing CHI3L1 significantly induced VSMCs apoptosis (see Fig 16), and simultaneously significantly inhibited VSMC proliferation (see Fig 17) and migration (Fig 15). Likewise, at least partly in agreement with our findings, a recent study found that silencing CHI3L1 in primary cultured mouse aortic VSMC from C57BL/6 mice aorta reduced PDGF-BB-stimulated VSMC migration and proliferation (Jung 2018). However, there were no significant differences observed in VSMC survival induced by CHI3L1 overexpression. Interestingly, studies in human bronchial smooth muscle cells (BSMCs) indicated that increased CHI3L1 can induced BSMC proliferation and migration by either producing IL-8 or through PAR-2-, AKT-, and ERK-dependent mechanism (Bara2012) (Tang2012). Additionally, CHI3L1 pig homolog (gp38k) can

regulate SMC migration, adhesion, and spreading in VSMC derived from thoracic aortic explants of adult pigs. Thus, reports linking CHI3L1 with VSMC behavior suggest that CHI3L1 can regulate VSMC cell fate but may vary dramatically depending on different SMC origin and pathophysiological conditions.

To date, few studies have explored CHI3L1's functional role and underlying mechanism in VSMCs. In this present work, we identified that Krueppel-like factor 4 (KLF4), which research groups have previously shown plays a vital role in regulating VSMC phenotypic switching, VSMC functional properties and overall plaque pathogenesis (Yoshida 2008) (Deaton 2009) is associated with CHI3L1 knockdown modulation in VSMCs (see Fig 18). Furthermore, our results of trans-differentiation demonstrated that silencing CHI3L1 can significantly suppress mRNA expression of VSMC markers ACTA2 (α -SMA) and simultaneously increase mRNA expression of macrophages markers CD68 (see Fig 14). Therefore, we postulated that the knockdown of CHI3L1 within VSMC results in VSMC trans-differentiation through the regulatory role of KLF4.

Meanwhile, it is noteworthy that MyoG was detected significantly associated with CHI3L1-modulation in VSMCs (see Fig 14). A key regulator of skeletal muscle gene expression, MyoG, and together with MyoD, another muscle-specific myogenic regulatory factor (MRF), has been considered] dominant over the differentiation of SMC (Long 2007). This compelling study demonstrated that MyoD, rather than be a coactivator that induces VSMC differentiation via stimulating serum response factor (SRF) dependent smooth muscle cell marker, can function as a repressor of MyoG, inhibiting skeletal muscle cell differentiation. Since muscle-derived stem cells or skeletal myoblasts expressing MyoG are refractory to terminal differentiation, obtaining an SMC-like phenotype and further becoming a functional SMC, we assumed that MyoG is also involved in the development of atherosclerosis, directly inhibiting skeletal muscle cell differentiation while promoting SMC differentiation. Collectively, we boldly hypothesized that reduced MyoG mediated by CHI3L1 can directly inhibit skeletal muscle differentiation while activating SMC phenotype.

Unfortunately, we were not able to identify genes significantly associated with VSMC survival due to the small number of specified candidates on our custom gene expression array plate. Although CDKN1A (p21) and p53 seemed to be mediated by CHI3L1 from the analysis (see Fig 18), a large-scale unbiased gene expression profiling or specific arrays containing genes related to pathway of VSMC proliferation/apoptosis/migration should be designed and explored. Lastly, through in silico analysis of the putative transcription factor, CREBP1 was reported as the highest possible transcription factor of CHI3L1 by showing the highest matching score and having both DNA methylation marks and single nucleotide polymorphisms in its TF-DNA binding area. However, further experiments, such as chromatin immunoprecipitation and Luciferase reporter assay should be performed to confirm this result.

It should be mentioned that this project actually included an *in vivo* study aiming to explore the function role of CHI3L1 in vascular remodeling and plaque vulnerability, which was predominantly completed by Pavlos Tsantilas, a Vascular Surgeon from our Clinic, at our cooperative laboratory in Stanford University. They established two animal models that investigate vascular remodeling and plaque vulnerability, respectively, in four different background mice, including *Chi3l1*^{-/-} *Cre/FloxP*, *C57BL6* (Wildtype), *ApoE*^{-/-}, and *Myh11/Tom*^{-/+} mice. Consequently, they observed that inhibiting CHI3L1 can increase total vessel area and its individual components (media, intima and lumen). Meanwhile, the percentage of α SMA⁺ cells in the intima was reduced in the remodeling model, and the percentage of α SMA⁺ cells was significantly reduced in the fibrous cap within advanced lesions in the vulnerability model. This *in vivo* work is of great complimentary value to the *in vitro* and *ex vivo* studies presented in my thesis. Further explorations and studies will shed light on the molecular mechanisms through which CHI3L1 induces VSMC dynamics, such as migration, proliferation, and apoptosis. One final limitation is that our *in vitro* study was limited by a relatively small sample size when utilizing cells being derived from patients. Here obviously a better characterization of the patients from which the cells originate from is needed, and more cells from further patients should be generated.

5. SUMMARY

In conclusion, the present study provides evidence that CHI3L1 plays a role in VSMC-mediated advancement of atherosclerosis. *Ex vivo* results demonstrate that anti-CHI3L1 immuno-expression in the areas populated by VSMC are increased in rupture plaques. Further, the *in vitro* study demonstrated that CHI3L1 exerts effects on VSMC cell fate decisions, with the ability to induce cell apoptosis and reduce cell migration/proliferation as well. Intriguingly, gene array analysis found two VSMC-trans-differentiation-related genes – KLF4 and MyoG – were associated with CHI3L1 modulation. At the same time, inhibiting CHI3L1 might result in smooth muscle cell trans-differentiation by altering the expression patterns of macrophage and VSMC markers. Last, if I am allowed to mention our cooperator-based *in vivo* data, CHI3L1 seemingly prevents VSMC dedifferentiation and transformation in the vasculature by increasing α SMA-expression in intima of vascular remodeling mice model and in the fibrous cap of an inducible plaque vulnerability model. Collectively, our studies can be interpreted as evidence that CHI3L1 contributes to VSMC-mediated atherosclerotic plaque pathogenesis.

6. REFERENCES

- (Adamson 2015) Adamson PD, Dweck MR, Newby DE: The vulnerable atherosclerotic plaque: in vivo identification and potential therapeutic avenues. *Heart*, 2015; 1: 1-12.
- (Allahverdian 2014), Allahverdian S, Chehroudi AC, McManus BM, Abraham T, Francis GA: Contribution of intimal smooth muscle cells to cholesterol accumulation and macrophage-like cells in human atherosclerosis. *Circulation*, 2014; 129: 1551-1559.
- (Alexander 2012) Alexander MR, Owens GK: Epigenetic control of smooth muscle cell differentiation and phenotypic switching in vascular development and disease. *Annu Rev Physiol*, 2012;74:13-40.
- (Bara 2012) Bara I, Ozier A, Girodet PO, Carvalho G, Cattiaux J, Begueret H, Thumerel M, Ousova O, Kolbeck R, Coyle AJ, Woods J, Tunon de Lara JM, Marthan R, Berger P: Role of YKL-40 in Bronchial Smooth Muscle Remodeling in Asthma. *American Journal of Respiratory and Critical Care Medicine*, 2012; 185: 715-722.
- (Benjamin 2018) Benjamin, EJ, Virani SS, Callaway CW, Chamberlain AM: Heart disease and stroke statistics-2018 update: A report from the American Heart Association. *Circulation*, 2018; 137, e67-e492.
- (Bennett 2016) Bennett, MR, S Sinha, GK Owens:Vascular Smooth Muscle Cells in Atherosclerosis. *Circ Res*, 2016; 118: 692-702.
- (Bentzon JF 2014)Bentzon JF, Otsuka F, Virmani R, Falk E: Mechanisms of plaque formation and rupture. *Circ Res*, 2014; 114: 1852-66.
- (Bhat 2008) Bhat KP, Pelloski CE, Zhang Y, Kim SH: Selective repression of YKL-40 by NF- κ B in glioma cell lines involves recruitment of histone deacetylase-1 and -2. *FEBS Lett*, 2008; 582: 3193-200.
- (Bleau 1999) Bleau G, Massicotte F, Merlen Y, Boisvert C: Mammalian chitinase-like proteins, 1999; *EXS* 87:211-21.
- (Bonneh-Barkay 2010) Bonneh-Barkay D, Wang G, Starkey A, Hamilton RL, Wiley CA: In vivo CHI3L1 (YKL-40) expression in astrocytes in acute and chronic neurological diseases. *J Neuroinflammation*, 2010;7: 34-41.
- (Boot 1999) Boot RG, van Aken BE, Renkema GH, Jacobs MJ, Aerts JM, de Vries CJ: Strong induction of members of the chitinase family of proteins in atherosclerosis: chitotriosidase and human cartilage gp-39 expressed in lesion macrophages. *Arteriosclerosis, Thrombosis, and Vascular Biology*, 1999,19(3): 687-694.
- (Caplan 2009) Caplan LR: Chapter2-Basic pathology, anatomy, and pathophysiology of stroke. *Caplan's stroke(Fourth Edition)*: 22-63.
- (Catalan 2012) Catalan V: Role of extracellular matrix remodelling in adipose tissue pathophysiology: relevance in the development of obesity. *Histology and histopathology*, 2012; 27, 1515-1528.
- (Chen 2017) Chen XJ, Li Q, Xue J, Wang B, Jin KL, Shao B: Serum YKL-40, a prognostic marker in patients with large-artery atherosclerotic stroke, *Acta Neurol Scand*, 2017; 136: 97-102.
- (Cherepanova 2016) Cherepanova OA, Gomez D, Shankman LS, Swiatlowska P, Williams J: Activation of the pluripotency factor OCT4 in smooth muscle cells in atheroprotective. *Nat Med*, 2016; 22(6): 657-665.
- (Creager 2004) Creager MA: Atherosclerotic Vascular Disease Conference: Writing Group V:

medical decision making and therapy. *Circulation*, 2014; 109: 2634-2642.

(del Zoppo 2006) del Zoppo GJ: Stroke and neurovascular protection. *The New England journal of medicine*, 2006; 354,553-555.

(Di Rosa 2016) Di Rosa M: CHI3L1 nuclear localization in monocyte derived dendritic cells. *Immunobiology*, 2016; 22: 347-356.

(Di Rosa 2016) Di Rosa M: Chitinase 3 Like-1: An Emerging Molecule Involved in Diabetes and Diabetic Complications. *Pathobiology*, 2016; 83: 228-242.

(Deaton 2009) Deaton RA, Gan Q, Owens GK: Sp1-dependent activation of KLF4 is required for PDGF-BB-induced phenotypic modulation of smooth muscle. *Am. J. Physiol. Heart Circ. Physiol*, 2009,296, H1027–H1037.

(Executive Committee for the Asymptomatic Carotid Atherosclerosis Study 1995). Endarterectomy for asymptomatic carotid artery stenosis. *JAMA*, 1995; 273: 1421-8.

(Forbes 2011) Forbes SA: COSMIC: mining complete cancer genomes in the catalogue of somatic mutation in cancer. *Nucleic Acids Res*, 2011; 39 (Database issue): D945-D950.

(Feil 2014) Feil S, Fehrenbacher B, Lukowski R, Essmann F, Schulze-Osthoff K, Schaller M, Feil R: Transdifferentiation of vascular smooth muscle cells to macrophage-like cells during atherogenesis. *Circ. Res*, 2014, 115, 662-667.

(GBD 2015 DALYs and HALE Collaborators 2015) GBD 2015 DALYs and HALE Collaborators: Global, regional, and national disability-adjusted life-years (DALYS) for 315 diseases and injuries and healthy life expectancy (HALE), 1990-2015: a systematic analysis for the global burden of disease study 2015. *Lancet*, 2016; 388: 1603-1658.

(Glisic 2017) Glisic M, Mujaj B, Rueda-Ochoa OL, Asllanaj E, Laven JSE: Associations of Endogenous Estradiol and Testosterone Levels with Plaque Composition and Risk of Stroke in Subjects with Carotid Atherosclerosis. *Circ Res*, 2018; 122(1): 97-105.

(Go 2014) Go AS: Executive summary: heart disease and stroke statistics-2014 update: a report from the american heart association. *Circulation*, 2014;129(3): 399-410.

(Hankey 2017) Hankey GJ: Stroke. *Lancet*, 2017; 389(10069): 641-654.

(Hatsukami 2000) Hatsukami TS, Ross R, Polissar NL, Yuan C: Visualization of fibrous cap thickness and rupture in human atherosclerotic carotid plaque in vivo with high-resolution magnetic resonance imaging. *Circulation*, 2000; 102(9): 959-64.

(Hobson 2008) Hobson RW, Mackey WC, Ascher E, Murad MH, Calligaro KD, Comerota AJ: Management of atherosclerotic carotid artery disease: clinical practice guidelines of the Society for Vascular Surgery. *J Vasc Surg*, 2008; 48(2): 480-486.

(Huang 2018) Huang H, Zheng J, Shen N, Wang G, Zhou G, Fang Y, Lin J, Zhao J: Identification of pathways and genes associated with synovitis in osteoarthritis using bioinformatics analyses. *Scientific reports*, 2018; 8:10050.

(Johansen 1992) Johansen JS, Williamson MK, Rice JS, Price PA: Identification of proteins secreted by human osteoblastic cells in culture. *J Bone Miner Res*, 1992: 501-512.

(Johansen 2006) Johansen, JS: Studies on serum YKL-40 as a biomarker in diseases with inflammation, tissue remodelling, fibroses and cancer. *Dan Med Bull*, 2006; 53: 172-209.

(Joseph 2017) Joseph Philip, Leong D, McKee M, Anand SS, Schwalm JD, Teo K, Mentz A, Yusuf S: Reducing the Global Burden of Cardiovascular Disease, Part 1, The Epidemiology and Risk Factors. *Circ Res*, 2017; 121: 677-694.

(Jung 2018) Jung YY, Kim KC, Park MH, Seo Y, Park H, Park MH, Chang J: Atherosclerosis is

exacerbated by chitinase-3-like-1 in amyloid precursor protein transgenic mice. *Theranostics*, 2018;1; 8(3): 749-766.

(Kamba 2013) Kamba A, Lee IA, Mizoguchi E: Potential association between TLR4 and chitinase 3-like-1 (CHI3L1/YKL-40) signaling on colonic epithelial cells in inflammatory bowel disease and colitis-associated cancer. *Curr Mol Med*, 2013; 13: 1110-1121.

(Kastrup 2009) Kastrup J, Johansen JS, Winkel P, Hansen JF, Hildebrandt P, Jensen GB, Jespersen CM: High serum YKL-40 concentration is associated with cardiovascular and all-cause mortality in patients with stable coronary artery disease. *Eur Heart J*,2009;30:1066-107.

(Kjaergaard 2010) Kjaergaard AD, Bojesen SE, Johansen JS, Nordestgaard BG: Elevated plasma YKL-40 levels and ischemic stroke in the general population. *Ann Neurol*, 2010; 68: 672-680.

(Kjaergaard 2010) Kjaergaard AD, Johansen JS, Bojesen SE, Nordestgaard BG: Elevated plasma YKL-40, lipids and lipoproteins, and ischemic vascular disease in the general population. *Stroke*, 2015; 46: 329-335.

(Kjaergaard 2016) Kjaergaard AD, Johansen JS, Bojesen SE, Nordestgaard BG: Observationally and Genetically High YKL-40 and Risk of Venous Thromboembolism in the General Population. *Arteriosclerosis, Thrombosis, and Vascular Biology*, 2016;36:1030-1036.

(Kolodgie 2001) Kolodgie FD, Burke AP, Farb A, Gold HK, Yuan J, Narula J, Finn AV, Virmani R: The thin-cap fibroatheroma: a type of vulnerable plaque: the major precursor lesion to acute coronary syndromes. *Curr Opin Cardiol*, 2001;16: 285-292.

(Kim 2018) Kim KC, Yun J, Son DJ, Kim JY, Jung JK, Choi JS, Kim YR: Suppression of metastasis through inhibition of chitinase-3-like 1 expression by miR-125a-3p-mediated up-regulation of USF1. *Theranostics*, 2018; 8(16): 4409-4428.

(Lee 2009) Lee CC, Hartl D, Lee GR, Koller B, Matsuura H, Da Silva CA: Role of breast regression protein 39 (BRP-39)/chitinase 3-like-1 in Th2 and IL13-induced tissue responses and apoptosis. *J Exp Med*, 2009; 206(5): 1149-66.

(Lee 2011) Lee Chun Geun, Da Silva CA, Dela Cruz CS, Ahangari F, Ma B: Role of Chitin and Chitinase/Chitinase-Like Proteins in Inflammation, Tissue Remodeling, and Injury. *Annu. Rev. Physiol*, 2011; 73: 479-501.

(Leeper 2018) Leeper NJ, Maegdefessel L: Non-coding RNAs: key regulators of smooth muscle cell fate in vascular disease. *Cardiovascular Research*, 2018; 114(4): 611-621.

(Li 2016) Li Z, Du L, Wang F, Luo X: Assessment of the arterial stiffness in patients with acute ischemic stroke using longitudinal elasticity modulus measurements obtained with Shear Wave Elastography. *Med Ultrason*, 2016; 18: 182-189.

(Li 2018) Li Z, Bai Y, Li W, Gao F, Kuang Y, Du L, Luo X: Carotid vulnerable plaques are associated with circulating leukocytes in acute ischemic stroke patients: an clinical study based on contrast-enhanced ultrasound. *Sci Rep*, 2018; 8(1): 8849.

(Li 2018) Li DY, Busch A, Jin H, Chernogubova E, Pelisek J, Karlsson J, Sennblad B, Liu S, Lao S: H19 Induces Abdominal Aortic Aneurysm Development and Progression. *Circulation*, 2018; 138(15): 1551-1568.

(Libby 2011) Libby P, Ridker PM, Hansson GK: Progress and challenges in translating the biology of atherosclerosis. *Nature*, 2011; 473, 317-325.

(Liem 2017) Liem MI, Kennedy F, Bonati LH, van der Lugt A, Coolen BF, Nederveen AJ: Investigations of Carotid Stenosis to Identify Vulnerable Atherosclerotic Plaque and Determine Individual Stroke Risk. *Circ J*, 2017; 81(9): 1246-1253.

(Ling 2004) Ling H, Recklies AD: The chitinase 3-like protein human cartilage glycoprotein 39 inhibits cellular responses to the inflammatory cytokines interleukin-1 and tumour necrosis factor alpha. *Biochem J*, 2004; 380: 651-659.

(Maegdefessel 2014) Maegdefessel L: The emerging role of microRNAs in cardiovascular disease. *Journal of internal medicine*, 2014; 276, 633-644.

(Maegdefessel 2014) Maegdefessel L, Spin JM, Raaz U, Eken SM, Toh R, Azuma J, Adam M: miR-24 limits aortic vascular inflammation and murine abdominal aneurysm development. *Nat Commun*, 2014, 31; 5:5214.

(Matys 2006) Matys V: TRANSFAC and its module TRANS Compel: transcriptional gene regulation in eukaryotes. *Nuc Ac Res*, 2006; 34(Database issue): D108-110.

(Michelsen 2010) Michelsen AE, Rathcke CN, Skjelland M, Holm S, Ranheim T: Increased YKL-40 expression in patients with carotid atherosclerosis. *Atherosclerosis*, 2010; 211(2): 589-595.

(Millis 1985) Millis A.J.T, Hoyle M, Reich E, Mann DM: Isolation and characterization of a Mr 38,000 protein from differentiating smooth muscle cells. *J. Biol. Chem*, 1985; 260: 3754-3761.

(Moresi 2010) Moresi V, Williams AH, Meadows E, Flynn JM, Potthoff MJ, McAnally J, Shelton JM: Myogenin and class II HDACs control neurogenic muscle atrophy by inducing E3 ubiquitin ligases. *Cell*, 2010; 143(1): 35-45.

(Moulton 1999) Moulton KS, Heller E, Konerding MA, Flynn E, Palinski W: Angiogenesis inhibitors endostatin or TNP-470 reduce intimal neovascularization and plaque growth in apolipoprotein E-deficient mice. *Circulation*, 1999; 99: 1726-1732.

(Morozov 2013) Morozov VY, Ioshikhes IP: Optimized Position Weight Matrices in Prediction of Novel Putative Binding Sites for Transcription Factors in the *Drosophila melanogaster* Genome. *Plos one*, 2013; 8(8): e68712.

(Mughal 2011) Mughal MM, Khan MK, DeMarco JK, Majid A, Shamoun F, Abela GS: Symptomatic and asymptomatic carotid artery plaque. *Expert Rev Cardiovasc Ther*, 2011; 9: 1315-1330.

(Muller 1989) Muller JE, Tofler GH, Stone PH: Circadian variation and triggers of onset of acute cardiovascular disease. *Circulation*, 1989; 79: 733-743.

(Naghavi 2003) Naghavi M: From Vulnerable Plaque to Vulnerable Patient: A Call for New Definitions and RiskAssessment Strategies: Part I. *Circulation*, 2003;108: 1664-1672.

(Nishikawa 2003) Nishikawa KC, Millis AJ: gp38k (CHI3L1) is a novel adhesion and migration factor for vascular cells. *Exp Cell Res*, 2003; 287:79-87.

(Nojgaard 2008) Nojgaard C, Høst NB, Christensen IJ, Poulsen SH, Egstrup K, Price PA, Johansen JS: Serum levels of YKL-40 increases in patients with acute myocardial infarction. *Coron Artery Dis*, 2008; 19: 257-263.

(North American Symptomatic Carotid Endarterectomy Trial Collaborators 1991). Beneficial effect of carotid endarterectomy in symptomatic patients with high-grade carotid stenosis. *N Engl J Med*, 1991; 325: 445-53.

(Park 2012) Park HY, Jun CD, Jeon SJ, Choi SS, Kim HR: Serum YKL-40 Levels Correlate with Infarct Volume, Stroke Severity, and Functional Outcome in Acute Ischemic Stroke Patients. *PLoS One*, 2012; 7(12): e51722.

(Pelisek 2019) Pelisek J, Hegenloh R, Bauer S, Metschl S, Pauli J, Glukha N: Biobanking: Objectives, Requirements, and Future Challenges Experiences from the Munich Vascular Biobank. *J Clin Med*, 2019; 16;8(2).

(Perisic 2016) Perisic L, Aldi S, Sun Y, Folkersen L, Razuvaev A, Roy J: Gene expression signature, pathway and networks in carotid atherosclerosis. *Atherosclerosis*, 2016; 279(3): 293-308.

(Phillips 2006) Phillips HS, Kharbanda S, Chen R, Forrest WF, Soriano RH, Wu TD, Misra A: Molecular subclasses of high-grade glioma predict prognosis, delineate a pattern of disease progression, and resemble stages in neurogenesis. *Cancer Cell*, 2006; 9: 157-173.

(Rathcke 2009) Rathcke CN, Vestergaard H: YKL-40 - an emerging biomarker in cardiovascular disease and Diabetes. *Cardiovascular Diabetology*, 2009; 8: 61-68.

(Recklies 2005) Recklies AD, Ling H, White C, Bernier SM: Inflammatory cytokines induce production of CHI3L1 by articular chondrocytes. *J Biol Chem*, 2005; 280: 41213-41221.

(Redgrave 2006) Redgrave JN, Lovett JK, Gallagher PJ, Rothwell PM: Histological assessment of 526 symptomatic carotid plaques in relation to the nature and timing of ischemic symptoms: The Oxford plaque study. *Circulation*, 2006; 113: 2320-2328.

(Rehli 2003) Rehli M, Niller HH, Ammon C, Langmann S, Schwarzfischer L, Andreesen R, Krause SW: Transcriptional regulation of CHI3L1, a marker gene for late stages of macrophage differentiation. *J Biol Chem*, 2003; 278: 44058-44067.

(Roslind 2009) Roslind Anne, Johansen JS: YKL-40: A Novel Marker Shared by Chronic Inflammation and Oncogenic Transformation. *Methods Mol Biol*, 2009; 511: 159-84.

(Roth 2015) Roth GA, Forouzanfar MH, Moran AE, Barber R: Demographic and epidemiologic drivers of global cardiovascular mortality. *N Engl J Med*, 2015; 372: 1333-1341.

(Ross 1999) Ross R: Atherosclerosis-an inflammatory disease. *N. Engl. J. Med*, 1999; 340, 115-126 .

(Ricci-Vitiani 2008) Ricci-Vitiani L, Pallini R, Larocca LM, Lombardi DG, Signore M: Mesenchymal differentiation of glioblastoma stem cells. *Cell Death Differ*, 2008; 15: 1491-1498.

(Rudolph 2010) Rudolph V, Andrié RP, Rudolph TK, Friedrichs K, Klinke A, Hirsch-Hoffmann B: Myeloperoxidase acts as a profibrotic mediator of atrial fibrillation. *Nat Med*, 2010; 16, 470-474.

(Shankman 2015) Shankman LS: KLF4 dependent phenotypic modulation of SMCs plays a key role in atherosclerotic plaque pathogenesis. *Nat med*, 2015; 21(6): 629-637.

(Schrijvers 2005) Schrijvers DM, De Meyer GR, Kockx MM, Herman AG: Phagocytosis of apoptotic cells by macrophages is impaired in atherosclerosis. *Arterioscler Thromb Vasc Biol*, 2005; 25:1256-1261.

(Shao2014) Shao Rong, Francescone R, Ngernyuang N, Bentley B: Anti-YKL-40 antibody and ionizing irradiation synergistically inhibit tumor vascularization and malignancy in glioblastoma. *Carcinogenesis*, 2014; 35(2): 373-382.

(Sohn 2009) Sohn MH, Kang MJ, Matsuura H, Bhandari V, Chen NY, Lee CG, Elias JA: The Chitinase-like Proteins Breast Regression Protein-39 and YKL-40 Regulate Hyperoxia-induced Acute Lung Injury. *Am J Respir Crit Care Med*, 2010; 1; 182(7): 918-28.

(Spagnoli 2004) Spagnoli LG, Mauriello A, Sangiorgi G, Fratoni S, Bonanno E, Schwartz RS, Piepgras DG: Extracranial thrombotically active carotid plaque as a risk factor for ischemic stroke. *JAMA*, 2004; 292: 1845-1852.

(Stary 1995) Stary HC, Chandler AB, Dinsmore RE, Fuster V, Glagov S, Insull W Jr: A definition of advanced types of atherosclerotic lesions and a histological classification of atherosclerosis: a report from the Committee on Vascular Lesions of the Council on Arteriosclerosis, American Heart Association. *Circulation*, 1995; 92: 1355-1374.

(Tang 2012) Tang H, Sun Y, Shi Z, Huang H, Fang Z, Chen J, Xiu Q, Li B: YKL-40 Induces IL-8

Expression from Bronchial Epithelium via MAPK (JNK and ERK) and NF- κ B Pathways, Causing Bronchial Smooth Muscle Proliferation and Migration. *J Immunol*, 2013; 190: 438-446.

(Vengrenyuk 2015) Vengrenyuk Y, Nishi H1, Long X1, Ouimet M1, Savji N1, Martinez FO1, Cassella CP: Cholesterol loading reprograms the microRNA-143/145-myocardin axis to convert aortic smooth muscle cells to a dysfunctional macrophage-like phenotype. *Arterioscler Thromb Vasc Biol*, 2015; 35: 535-546.

(Virmani 2000) Virmani R, Kolodgie FD, Burke AP, Farb A, Schwartz SM: Lessons from sudden coronary death: a comprehensive morphological classification scheme for atherosclerotic lesions. *Arterioscler Thromb Vasc Biol*, 2000; 20: 1262-1275.

(Wheeler 2007) Wheeler DL: Database resources of the national center for biotechnology information. *Nucleic Acids Res*, 2007; 35(Database issue): D5-D12.

(Xu 2018) Xu S, Kamato D, Little PJ, Nakagawa S, Pelisek J: Targeting epigenetics and non-coding RNAs in atherosclerosis: from mechanisms to therapeutics. *Pharmacol Ther*, 2019; 196: 15-43.

(Yu 2012) Yu W, Zhang Y, Xu L, Sun S, Jiang X, Zhang F: Microarray-based bioinformatics analysis of osteoblasts on TiO₂ nanotube layers. *Colloids Surf B Biointerfaces*, 2012; 93: 135-142.

(Yoshida 2008) Yoshida T, Kaestner KH, Owens GK: Conditional deletion of Krüppel-like factor 4 delays downregulation of smooth muscle cell differentiation markers but accelerates neointimal formation following vascular injury. *Circ. Res*, 2008, 102, 1548-1557.

(Zivin 2012) Zivin JA, Lee Goldman Andrew Schafer: *Ischemic Cerebrovascular Disease Goldman's Cecil Medicine: Twenty Fourth Edition*. 2012: 2310-2320.

7. APPENDIX

7.1 Abbreviations

α -SMA	Alpha smooth muscle actin
AIS	Acute Ischemic Stroke
Apoe ^{-/-}	Apolipoprotein E knockout
BiKE	Biobank of Karolinska Endarterectomies
CHI3L1	Chitinase-3-like-protein-1
CHI3L1 ^{-/-} Cre/FloxP transgenic mouse	Chitinase-3-like-protein-1 knockout CreLoxP-inducible transgenic mouse
CLP	Chitinase-like-protein
CVD	Cardiovascular diseases
CDKN1A	Cyclin Dependent Kinase Inhibitor 1A, p21
Col	Collagen
ECM	extracellular matrix
FFPE	fixed with formaldehyde and embedded in paraffin
FN	fibronectin
GCBI	Gene Cloud of Biotechnology Information
HCtSMC	Human carotid artery smooth muscle cell
IHD	ischemic heart disease
IPH	intraplaque hemorrhage
LAA	large-artery atherosclerosis
LCM	Laser capture microdissection
LN	laminin
MVB	Munich Vascular Biobank
M Φ	macrophage
MyoG	myogenin
MMPs	matrix metalloproteinases
Myh11/Tom ^{-/+}	Myh11/Tomato transgenic mouse
POU5F1	POU Class 5 Homebox 1, Oct4
PWM	position weight matrice
RHD	rheumatic heart disease
SNPs	single nucleotide polymorphisms
siRNA	small interfering RNA
TSS	transcription start site
TFBS	transcription factor binding sites
TIMPs	tissue inhibitors of MMPs
TP53	tumor protein p53

7.2 Publications

7.2.1 Original publications

Shen Lao, Jing Xu, Yunqi Liu, Songwang Cai. Comparative study on influences of two kinds of PHEMA stents on differentiation of ASCs into myocardial cells. *Mol Med Rep*, 2017; 16(1): 507-514.

Li DY, Busch A, Jin H, Chernogubova E, Pelisek J, Karlsson J, Sennblad B, Liu S, **Lao S**, Hofmann P, Bäcklund A, Eken SM, Roy J, Eriksson P, Dacken B, Ramanujam D, Dueck A, Engelhardt S, Boon RA, Eckstein HH, Spin JM, Tsao PS, Maegdefessel L. H19 Induces Abdominal Aortic Aneurysm Development and Progression. *Circulation*, 2018, 9; 138(15): 1551-1568.

7.2.2 Oral & Poster Presentation

Shen Lao, Pavlos Tsantilas, Monika Vaerst, Yuhuang Li, Vivek Nanda¹, Ying Wang, Yoko Kojima, Jianqin Ye, Alyssa Flores, Kai-Uwe Jarr, Jaroslav Pelisek, Hans-Henning Eckstein, Lars Maegdefessel, Nicholas Leeper. 8th Munich Vascular Conference 2018, Munich, Germany

CHI3L1 and Its Role in Vascular Smooth Muscle Cell Proliferation and Migration in Advanced Atherosclerosis. Pavlos Tsantilas, **Shen Lao**, Monika Vaerst, Yuhuang Li, Vivek Nanda, Lars Maegdefessel, Nicholas Leeper. Arteriosclerosis, Thrombosis and Vascular Biology Conference 2018, San Francisco, USA

Pavlos Tsantilas, **Shen Lao**, Monika Vaerst, Yuhuang Li, Vivek Nanda¹, Ying Wang, Yoko Kojima, Jianqin Ye, Alyssa Flores, Kai-Uwe Jarr, Jaroslav Pelisek, Hans-Henning Eckstein, Lars Maegdefessel, Nicholas Leeper. Chitinase-3-like Protein 1 is an Inhibitor of Vascular Smooth Muscle Cell Dedifferentiation in Advanced Atherosclerosis. Arteriosclerosis, Thrombosis and Vascular Biology Conference 2019, Boston, USA

7.3 Acknowledgments

This present dissertation marks the end of my journey to obtain the M.D title. Working at Lars group has been an unforgettable learning experience. It's my great pleasure and honor to express my sincere thanks to all those who have contributed to the success of this thesis work.

First and foremost I wish to thank my lovely advisor, Prof. Dr. med. Lars Maegdefessel, director of the Vascular Biology and Experimental Vascular Medicine Unit, who is an enthusiastic, energetic leader and the funniest advisor and one of the smartest people I met. His knowledge, judgment, and patience guided me during the entire time.

I would also like to thank my mentor, Asst. Prof. Dr. PhD. Alexandra Baecklund, for her valuable guidance. Further, I am very thankful to Prof. Dr. rer. nat. Jaroslav Pelisek, head of Munich Vascular Biobank, for his professional guidance and all the encouragement. He and Renate Hegenloh, who is medical lab technician works in our biobank, trained and helped me a lot on immunohistochemistry work.

Next, I want to thank Dr. med. PhD. Daniel Li. In the very beginning, I knew little about the basic research work concerning my MD project and he inducted me patiently in all techniques necessary to fulfil my thesis. I appreciate him not only for his technical help, but also for being good listener and supporter.

To our beautiful group leader and friend of mine as well, Dr. med. PhD. Valentina Paloschi, she has always been very understanding and patient with me. Thank you very much for your genuine enthusiasm, experience and encouragement.

I am also indebted to Asst. Prof. Nicholas Leeper, director of Vascular Research in Stanford University School of Medicine, for inviting me to visit his lab and providing an opportunity to discuss our collaborative research and exchange ideas, methodologies and techniques.

An equally important person I will forever be thankful is my talented collaborator, Dr. med. Pavlos Tsantilas, Clinician-Scientist of Vascular and Endovascular Surgery. He contributed a lot to this big project, not only perfectly completed all in vivo study concerning this project in Stanford but also advised me many constructive suggestions enabling us to make the continuous progress.

To my lovely colleagues, postdoc Francesca Fasolo, thanks for the kind technical support; Sabine Bauer, PhD student, thanks for introducing me to the Qubit measurement; Hanna Winter, PhD student, thanks for introducing me to the Incucyte analysis; Jessica Pauli, PhD student, thank you for the preparation of paraffin sections;

Susanne Metschl, PhD student, Shengliang Liu, MD student, Zhiyuan Wu, MD student, and Nadiya Glukha, lab technician, thank you all for providing helpful suggestions and helping me with instrumentation and general lab questions during throughout the project process. I was so lucky to be a part of this lovely group.

Finally, I wouldn't have been able to finish this thesis without the tremendous help and unconditional love of my lovely family. Thanks for my hard-working parents for raising me and providing unconditional love and care.

My deepest and loving thanks go to Jing Xu, my best friend, soul-mate and wife, who has sacrificed her live to raise our lovely daughter Sera. They are two most important women in my life. There are no words to convey how much I love them. The past several years have not been an easy ride, both academically and personally. I truly thank Jing and Sera for sticking by my side, even when I was irritable and depressed.

I believe that those rich scientific and cultural experiences I learn from this great country here in Germany will enable me to fulfill my ultimate goal of becoming a clinician-scientist in the field of cardiovascular surgery and being a better man with more responsibility.

7.4 Funding

Shen Lao (Award File No.201708080072) received a two-year scholarship of the China Scholarship Council (CSC). The funders were not involved in the study design, data collection and analysis, decision to publish, or preparation of the manuscript.